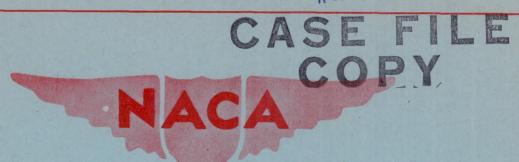
RESTRICTED

N 62 59 1 4RM No. L6L11



## RESEARCH MEMORANDUM

WIND-TUNNEL INVESTIGATION OF WING INLETS
FOR A FOUR-ENGINE AIRPLANE

Ву

Walter A. Bartlett, Jr. and Edwin B. Goral

Langley Memorial Aeronautical Laboratory

Langley Field, Va.

CLASSIFICATION CANCELLED

AUTHORITY DRYDEN 9-16-52

CLASSIFIED DOCUMENT

This document contains classified information affecting the National Defense of the United States within the meaning of the Emplomage Act, USC 50:31 and 32. Its transmission or the reveilation of its contents in any manner to an unauthorized person is pro-hibited by law, information so classified may be imparted only to persons in the military and naval services of the United States, appropriate only to person and employees of the Federal Government who have a legitimate interest therein, and to United States ottomate interest therein, and to United States of Received The States of Received States of State

CHANGE #766 W.H.L.

# NATIONAL ADVISORY COMMITTEE FOR AERONAUTICS

WASHINGTON March 11, 1947

RESTRICTED

CLASSIFICATION CANCELED

#### NATIONAL ADVISORY COMMITTEE FOR AERONAUTICS

#### RESEARCH MEMORANDUM

WIND-TUNNEL INVESTIGATION OF WING INLETS

FOR A FOUR-ENGINE AIRPLANE

By Walter A. Bartlett, Jr. and Edwin B. Goral

#### SUMMARY

An investigation has been conducted in the Langley propellerresearch tunnel to develop wing-leading-edge inlets for location
between the inboard and outboard nacelles on each wing of a
four-engine airplane for the Army Air Forces. The investigation
included aerodynamic tests of the basic wing and the original inlet,
and the development by the NACA of wing inlets for two versions of
the airplane.

The original inlet was found to decrease the maximum lift coefficients and to have critical Mach numbers below those of the wing with the basic nose installed. The total-pressure recovery in the oil cooler ducts was poor regardless of the inlet installation. As the sharp expanding bend in this duct cannot be avoided, it is recommended that the oil-cooler air be induced through the cowling or from some source other than the subject wing inlet.

Two inlets (nos. 5 and 6) were developed that should be satisfactory for the airplane. The maximum lift coefficients for the model with inlets 5 and 6 installed were about 1.21 and 1.22, respectively, with 0° wing flaps and 1.87 and 2.00, respectively, with 65° wing flaps compared to corresponding values of 1.20 and 2.01 for the model equipped with the faired basic nose. The predicted critical Mach numbers for inlets 5 and 6 for the critical military-power high speed condition for an altitude of 40,000 feet were 0.63 and 0.64, respectively, as compared to 0.64 for the thickest section of the basic wing. Propeller operation (either right or left hand) caused appreciable increases in maximum lift coefficients and in the total pressures in the ducting.

#### INTRODUCTION

An investigation has been conducted in the Langley propellerresearch tunnel to develop satisfactory wing-leading-edge inlets for location between the inboard and outboard nacelles on each wing of a four-engine airplane for the Army Air Forces. This high-speed, long-range airplane is powered by four Pratt & Whitney R-4360 engines which drive four-blade right-hand tractor propellers. Oil-cooler, intercooler-cooling, and charge air are supplied to the engine installation through ducts leading from wing-leading-edge inlets located between the inboard and outboard nacelles; the cooling air is exhausted through flapped exits on the lower surface of each nacelle while the engine exhaust is discharged through the nacelle tail. To avoid penalizing the performance of the airplane, it was considered essential that the wing inlets used should not reduce the maximum lift coefficients or critical Mach numbers below those of the basic wing, should have low parasite drag, and should provide a high pressure recovery over the complete range of flight conditions.

A  $\frac{1}{h}$ -scale semispan model of the left wing of the airplane was used for the tests. The model was equipped with an end plate at the fuselage location to give a wing-lift distribution approximating that of the left wing of the actual airplane.

The investigation included propeller-removed tests of the model with the basic nose, the original inlet, and 5 inlets constructed by this Laboratory in the course of the development program. A previous investigation of wing-leading-edge inlets which served as a guide in the development of the inlets is presented in reference 1.

The configurations were compared by lift measurements, staticpressure surveys on the duct lips, total-pressure surveys in the
internal flow, and profile drag measured by the wake survey method.
Additional tests were conducted to determine the pressure distributions
on the upper and lower surface of the outboard nacelle, the effect
of the end plate on the lift characteristics, and the effect of
propeller operation (for both right-and left-hand rotation) on the
lift characteristics and on the internal total-pressure coefficients.

#### SYMBOLS

The symbols used in this report are:

c section drag coefficient (d/qoc)

 $C_L$  lift coefficient (L/q<sub>o</sub>S)

 $T_c$  thrust disk-loading coefficient  $(T/2q_oD^2)$ 

- c section chord, 3.517 feet at wing station 72.25
- d section drag, pounds per unit span
- D propeller diameter, 3.917 feet
- L lift, pounds
- q free-stream dynamic pressure, pounds per square foot
- S wing area, 45.235 square feet
- T propeller thrust, pounds
- F projected frontal area of wing corresponding to span of portion of inlet under consideration (measured perpendicular to chord and between center lines of divider vanes)

Inboard oil cooler	0.186
Inboard intercooler	.453
Inboard carburetor	.228
Outboard carburetor	.219
Outboard intercooler	.432
Outboard oil cooler	.164
Complete inlet	1.682

- H total pressure, pounds per square foot
- M<sub>cr</sub> predicted critical Mach number
- p static pressure, pounds per square foot
- Q quantity rate of flow, cubic feet per second
- V velocity, feet per second
- angle of attack of root chord, degrees, corrected for jet boundary by the relation  $\alpha = \alpha_{\rm test} 1.052 C_{\rm L}$
- δ wing-flap deflection with respect to the root chord, degrees
- H Po total-pressure coefficient

p - p <sub>o</sub>	static-pressure coefficient
FV <sub>O</sub>	flow coefficient
V <sub>1</sub>	inlet-velocity ratio

#### Subscripts:

c carburetor ducts

i inlet

I intercooler

o free stream

oil cooler

t complete inlet

A bar over a symbol denotes an average value,

#### MODEL AND TESTS

Model. - Drawings of the model and a general view of the model mounted in the tunnel are presented as figure 1; photographs of the double slotted wing flaps in the several test positions are shown in figure 2.

The wing inlet with which the present investigation is concerned was located between the inboard and outboard nacelles. This inlet was divided by vanes into six separate ducts that simulated those of the airplane forward of the front spar; these ducts are identified in figure 1. Behind the front spar, nonscale ducts conveyed the internal flow to suitable exits beneath the nacelles. Shutters were provided in the ducts just upstream of the exits to permit control of the internal flow.

Cross-sectional sketches of the six inlet configurations tested are shown in figure 3 superimposed on outlines of the basic airfoil contour. Ordinates for these inlets for wing stations 55.125 and 90.125 are given in tables I through VI. The inlet lips were

developed by connecting with a straight line the ordinates at equal percent chords at these two wing stations. Ordinates of the basic airfoil sections used in the wing are given in table VII. Inlet number 1 was the original inlet furnished with the model; considerations which led to the development of the remaining inlets are discussed under the section of the report entitled 'Results and Discussion".

Because the external surfaces of inlets 3 and 6 were thicker than the basic airfoil at the point where the inlets detached from the rest of the wing, they were faired with modeling clay from that point to the section of maximum thickness of the wing. Discontinuities existed in the internal lines of inlets 4 and 5 just in front of the point of detachment because it was necessary to maintain a reasonable initial diffuser angle. These discontinuities were not faired because of difficulties incurred in obtaining access to the inner portions of the model. A detail sketch showing the position of this discontinuity for inlet 5 relative to the pressure tubes at the measuring station is given in figure 4.

An electric motor of 100 horsepower was installed in each nacelle to drive the model propellers. A view of the right-hand set of model propellers installed is presented as figure 5; identical left-hand propellers were used in some tests to duplicate the slipstream conditions for the right wing. A comparison of the blade-form characteristics for these propellers with those for the Curtiss 1016 propeller (specified as full-scale airplane equipment at the start of the testing) is given in figure 6. With the test blade angle set at 27° at the 75-percent radius station, computations showed that the thrust-torque relationship and the radial load distribution for the model propellers very nearly duplicated those for the full-scale propellers. The propeller hubs were enclosed in spinners of elliptical sections.

Two sets of flush cowling flaps, (fig. 2(c) and 2(e)) were furnished with the model to permit control of the engine-cowling air flow. As preliminary tests indicated that changes in the cowling flow quantities did not cause measurable differences in the flow conditions at the wing duct inlet, only the "long" cowling flaps, which produced an inlet-velocity ratio of the order of 0.76, were used in the investigation.

Instrumentation and methods. Closely spaced flush orifices were installed in the inlet surface at wing stations 56.813, 69.750, and 88.281 on inlets 1 through 3, but only at station 69.750 on inlets 4 through 6 because preliminary tests indicated that the static-pressure distributions were essentially the same for the three wing sections. Total- and static-pressure tubes were installed at the pressure-measuring stations in the charge-air and intercooler-

cooling-air ducts of the several inlets (see fig. 1). Grids of total-pressure tubes were also installed in the oil-cooler ducts downstream of the duct bends at the entrances of these ducts to the nacelles. Total- and static-pressure tubes were installed in the inlet section of the oil-cooler ducts only for inlet number 1. Pressures in the wake of the model were measured by a survey rake (fig. 2(a)) located at a distance of 20 percent of the chord behind the trailing edge of the wing. Pressure belts (fig. 7 and reference 2) were used to measure the static pressure distributions on the nacelle surface. Pressures in the internal cowling flow were measured by means of total- and static-pressure tubes mounted at four equally spaced stations in the cowling exit.

All pressures over the inlet lips and within the wing ducts were recorded simultaneously by photographing a multitube manometer; other pressures were obtained visually from a second multitube manometer. The average total pressures at each measuring station in the internal ducting were obtained through averaging by integration the faired curves of the local values in both the horizontal and vertical directions. Internal flow quantities were obtained through averaging by integration the local flow velocities calculated from the pressures measured in the ducts. The value of flow coef-

ficient  $\frac{Q}{FV_O}$  given for individual oil-cooler, intercooler and

carburetor ducts, is for that segment of the inlet being considered, and may be higher or lower than the total flow coefficient for the complete inlet. To aid in the interpretation of the data, curves for converting inlet-velocity ratio  $\frac{V_1}{V}$  to total flow coef-

ficient  $\frac{Q_t}{F_t V_0}$  are given in figure 8 for all the inlets tested.

Lift measurements were obtained by means of the recording tunnel-balance system.

Tests. - The model was mounted at  $0^{\circ}$  dihedral for the tunnel tests. Jury struts allowed the model to be positioned at any geometric angle of attack between  $-8^{\circ}$  and  $23^{\circ}$ .

Preliminary tests were conducted with the number 1 inlet installed to determine settings for the wing duct exit shutters that would provide approximately uniform entrance velocities across the duct inlet. The exit shutter calibrations thus determined were used to set the inlet-velocity ratios for all other wing-inlet configurations. As the quantity of flow through the oil cooler ducts was measured only for the number 1 inlet, the flow quantities through the oil cooler ducts of the other configurations were obtained from the exit-shutter calibration; this procedure appeared to be justified on the

basis of the observed constancy of the flow through the other ducts for given shutter settings despite changes in the inlet configuration.

In tests to obtain aerodynamic data on the basic wing, a solid leading edge replaced the duct inlet and the duct exits were sealed. The lift characteristics of the model were determined through a geometric angle-of-attack range from -8° to 23° for wing flap deflections of 0°, 20°, 65°, and 65° with flaps continued under nacelles. The nacelle surface-pressure distributions were measured simultaneously with the lift at geometric angles of attack of 0°, 5°, 10°, and 15°. Wake surveys, for the determination of the section drag coefficients, were obtained at a geometric angle of attack of -2° behind model wing station 72.25.

The lift and section drag characteristics of the model with the various inlets installed were determined in the same manner as described in the preceding paragraph over a range of flow quantities through the various ducts.

Total-pressure recoveries and surface-pressure distributions with the various inlets installed on the model were measured over a range of flow and lift coefficients that would allow the coverage of the range of flight operations. Total-pressure recoveries were also measured in the propeller-installed conditions over a wide range of thrust coefficients.

All tests were conducted in wind velocities of about 100 miles per hour with 0° and 20° wing flap deflections, and 80 miles per hour with the 65° deflection. Corresponding Reynolds numbers based on the mean aerodynamic chord were about 3,000,000 and 2,400,000, respectively.

#### RESULTS AND DISCUSSION

Lift data are presented in figures 9 through 11; section drag coefficients for several of the configurations are compared in figure 12; surface-pressure distributions and predicted critical Mach numbers are given in figures 13 through 16; and pressure data obtained at the measuring stations in the ducting are presented in figures 17 through 19. The effects of propeller operation on the lift characteristics and on the pressure recoveries in one compartment of the inlet are shown in figures 11 and 20, respectively.

Basic model. - The maximum lift coefficients for the basic model with the duct exits sealed and faired were 1.20, 1.54, and 2.01 for wing flap deflections of 0°, 20°, and 65°. (See fig. 9.) Extending the flap under the nacelles as shown in figure 2(d) decreased the maximum lift coefficient with 65° flap deflections to 1.94. A similar decrease was reported in reference 3.

In the course of additional tests of this model in the Langley 19-foot pressure tunnel, a maximum lift coefficient of 1.39 was obtained for the basic model with 0° flaps at a test Reynolds number of about 4,500,000. A reflection plane was used in these tests in place of the end plate used in the present investigation. Data given in reference 4 indicate that the difference in end conditions would account for differences in maximum lift coefficient of the order shown. An end-condition correction supplementary to the standard corrections must be applied to the lift data in this report if these data are to be used for other than comparative purposes.

The section drag coefficients for the basic wing at  $\alpha = -2.4^{\circ}$ , computed from wake surveys by the method of reference 5, were 0.0077 at wing station 72.25 midway between the nacelles and 0.0072 at wing station 113.75 outboard of the outboard nacelle. (See fig. 12.)

Distributions of static pressure on the top and bottom surface of the outboard nacelle are shown in figure 13. These data show that a greater pressure difference across the cooling ducts could be obtained in cruising and climbing flight by locating the duct exits on the top of the nacelles rather than on the bottom where they are located at present.

Inlet number 1. Inlet number 1, the original inlet furnished with the model, had a large ratio of inlet height to maximum wing thickness, a lip-stagger angle of 16.5°, and a lower lip which extended well below the contour of the basic airfoil. (See fig. 3.)

Lift characteristics of the model with the number 1 inlet installed are presented as a function of angle of attack in figures 10(a) and 10(b) for flap deflections of 0° and 65°. Increases in the rate of flow caused consistent increases in C<sub>I</sub> for

the 0 wing flap configuration, but had little or no effect on for the 65 wing flap configuration. At the maximum rate of  $^{\rm L}_{\rm max}$ 

internal flow investigated, substitution of inlet number 1 for the basic nose caused large reductions in  $C_{\rm L}$  as shown in the following table:

basis of the observed constancy of the flow through the other ducts for given shutter settings despite changes in the inlet configuration.

In tests to obtain aerodynamic data on the basic wing, a solid leading edge replaced the duct inlet and the duct exits were sealed. The lift characteristics of the model were determined through a geometric angle-of-attack range from -8° to 23° for wing flap deflections of 0°, 20°, 65° and 65° with flaps continued under nacelles. The nacelle surface-pressure distributions were measured simultaneously with the lift at geometric angles of attack of 0°, 5°, 10°, and 15°. Wake surveys, for the determination of the section drag coefficients, were obtained at a geometric angle of attack of -2° behind model wing station 72.25.

The lift and section drag characteristics of the model with the various inlets installed were determined in the same manner as described in the preceding paragraph over a range of flow quantities through the various ducts.

Total-pressure recoveries and surface-pressure distributions with the various inlets installed on the model were measured over a range of flow and lift coefficients that would allow the coverage of the range of flight operations. Total-pressure recoveries were also measured in the propeller-installed conditions over a wide range of thrust coefficients.

All tests were conducted in wind velocities of about 100 miles per hour with 0° and 20° wing flap deflections, and 80 miles per hour with the 65° deflection. Corresponding Reynolds numbers based on the mean aerodynamic chord were about 3,000,000 and 2,400,000, respectively.

#### RESULTS AND DISCUSSION

Lift data are presented in figures 9 through 11; section drag coefficients for several of the configurations are compared in figure 12; surface-pressure distributions and predicted critical Mach numbers are given in figures 13 through 16; and pressure data obtained at the measuring stations in the ducting are presented in figures 17 through 19. The effects of propeller operation on the lift characteristics and on the pressure recoveries in one compartment of the inlet are shown in figures 11 and 20, respectively.

Basic model. - The maximum lift coefficients for the basic model with the duct exits sealed and faired were 1.20, 1.54, and 2.01 for wing flap deflections of 0°, 20°, and 65°. (See fig. 9.) Extending the flap under the nacelles as shown in figure 2(d) decreased the maximum lift coefficient with 65° flap deflections to 1.94. A similar decrease was reported in reference 3.

In the course of additional tests of this model in the Langley 19-foot pressure tunnel, a maximum lift coefficient of 1.39 was obtained for the basic model with 0° flaps at a test Reynolds number of about 4,500,000. A reflection plane was used in these tests in place of the end plate used in the present investigation. Data given in reference 4 indicate that the difference in end conditions would account for differences in maximum lift coefficient of the order shown. An end-condition correction supplementary to the standard corrections must be applied to the lift data in this report if these data are to be used for other than comparative purposes.

The section drag coefficients for the basic wing at  $\alpha = -2.4^{\circ}$ , computed from wake surveys by the method of reference 5, were 0.0077 at wing station 72.25 midway between the nacelles and 0.0072 at wing station 113.75 outboard of the outboard nacelle. (See fig. 12.)

Distributions of static pressure on the top and bottom surface of the outboard nacelle are shown in figure 13. These data show that a greater pressure difference across the cooling ducts could be obtained in cruising and climbing flight by locating the duct exits on the top of the nacelles rather than on the bottom where they are located at present.

<u>Inlet number 1.-</u> Inlet number 1, the original inlet furnished with the model, had a large ratio of inlet height to maximum wing thickness, a lip-stagger angle of 16.5°, and a lower lip which extended well below the contour of the basic airfoil. (See fig. 3.)

Lift characteristics of the model with the number l inlet installed are presented as a function of angle of attack in figures 10(a) and 10(b) for flap deflections of 0° and 65°. Increases in the rate of flow caused consistent increases in C<sub>I</sub> for max

the 0° wing flap configuration, but had little or no effect on CL for the 65° wing flap configuration. At the maximum rate of max

internal flow investigated, substitution of inlet number 1 for the basic nose caused large reductions in  $C_{\text{L}}$  as shown in the following table:

Inlet	δ (deg)	G <sub>t</sub> F <sub>t</sub> V <sub>o</sub>	C <sub>L</sub> max		
Basic nose	0	driver description	1.20		
Inlet no. 1	0	0.124	1.05		
Basic nose	65	gration across sales of	2.01		
Inlet no. 1	0)	0.136	1.74		

For  $\alpha$  = -2.4°, the section drag coefficients for wing station 72.25 with inlet 1 installed on the model (fig. 12) ranged from about 0.0107 at  $\frac{Q_t}{F_t V_0}$  = 0.06 to about 0.0097 at  $\frac{Q_t}{F_t V_0}$  = 0.130 as compared to the value of 0.0077 for the basic wing.

A representative static-pressure distribution over the surface of inlet number 1 at wing station 69.75 (fig. 14) shows that a high peak negative pressure occurred on the lower inlet lip at  $\frac{Q_t}{F_t V_0} = 0.057$  for  $C_L = 0.25$ , a condition corresponding to high-speed flight at low altitudes. A similar peak pressure occurred on the upper lip at  $\frac{Q_t}{F_t V_0} = 0.104$  for  $C_L = 0.45$ , a high-speed

condition for high-altitude flight. A number of modifications were made to the lip shapes, therefore, in an attempt to eliminate these pressure peaks. These modifications were made by filling the inlet lips to new contours for a span 2 inches on either side of wing station 69.75 and then fairing gradually spanwise into the original lip shape. The final modifications shown by dotted lines in figure 14 resulted in large reductions in the negative pressure peaks. The predicted critical Mach numbers for each lip (fig. 15) were computed according to the method of reference 6. The predicted critical Mach numbers for the inlet at  $\frac{Q_t}{F_t V_0} = 0.096$ , the flow ratio for

high-speed flight at military power at 40,000 feet, are compared in figure 16 with the envelope of critical Mach numbers for the desired airplane performance. At a C of approximately 0.4,

which corresponds to the high-speed flight condition at an altitude of 40,000 feet, the predicted critical Mach numbers for the inlet are shown to be much lower than the desired values.

Total-pressure distributions at the measuring stations in the internal ducting of inlet l are shown for high-speed and climb flight configurations (propeller removed) in figures 17 and 18, respectively. The total-pressure recoveries were satisfactory at the low flow and lift coefficient (fig. 17); but at the higher flow and lift coefficient (fig. 18), while the recoveries in the carburetor duct were satisfactory, considerable losses occurred in the lower half of the remaining ducts and throughout the oil-cooler ducts. The losses in the intercooler duct are attributed to separation of the flow from the lower lip of the inlet. while the low recoveries in the oil-cooler ducts were caused by excessive losses through the 90° bends shown in figure 1. Total-pressure measurements along the sides of the nacelles at the inlet showed that the boundary layer entering the oil-cooler ducts was comparatively thin and did not appear to be directly responsible for losses of the magnitude shown.

Lines of constant total-pressure recovery at the measuring station in the number 1 inlet are plotted as functions of  $\frac{Q}{FV_O}$  and  $C_L$  in figure 19(a) for the individual ducts. Superimposed on these curves are the operational flow limits required by airplane specifications. It is pointed out that the operational flow range of the oil-cooler ducts was not covered, as the required values of  $\frac{Q_O}{F_OV_O}$  were not obtainable with the high losses present in these ducts. The remaining ducts had fairly satisfactory total-pressure recoveries  $\frac{\overline{H} - P_O}{Q_O}$  over most of the operational range, except at combinations of high values of  $C_L$  and  $\frac{Q}{FV_O}$ .

Inlet number 2. In inlet number 2 (fig. 3), the lower lip was brought nearer to the chord line and the height of the inlet was reduced by about 10 percent below that of inlet 1 (thereby increasing the design inlet-velocity ratios) in an attempt to increase the critical speeds for the inlet; the stagger angle was increased from 16.5° to 26° in an attempt to improve the pressure recovery at high angles of attack.

The maximum lift coefficients  $\delta = 0^{\circ}$  were not obtained with the number 2 inlet installed (fig. lO(c)) as the geometric angle

of attack could not be increased above 23°. The highest values of C<sub>I</sub>, obtained were of the same order as those of inlet 1 for comparable flow coefficients. The critical speeds for this inlet even after development were of the same order as of the modified number 1 inlet over the range of desired airplane performance and flow ratios. (See figs. 14 and 15.) These tests indicated that even major modifications to this inlet would not improve the lift characteristics or critical speeds; consequently tests of this inlet were terminated in favor of subsequent designs.

Inlet number 3. In inlet number 3 (fig. 3) the inlet height was reduced approximately 25 percent below that of inlet 1 to further increase the design inlet-velocity ratios; the lips were extended forward about 3 inches to increase the fineness ratio of the inlet section and to reduce the internal diffuser angle. The lip stagger angle was increased from 16.5° to 25° as for inlet 2, and the nose of the upper lip was dropped closer to the chord line to regain some of the camber in the upper lip lost through the extension of the lips.

The maximum lift coefficient for inlet 3 at  $\delta = 0^{\circ}$  (fig. 10(d)) was equal to that for inlet 1 (fig. 10(a)) at the same flow coefficient  $\frac{Q_t}{F_t V_o} = 0.133$ , and the critical speeds of inlet 3

(figs. 14 and 15) were considerably higher. Tests of this inlet were terminated as the maximum lift characteristics obtained with inlet 2 installed showed no improvement over those for inlet 1.

Inlet number 4.- Previous experience indicated that increases in  $C_{\text{L}}$  can be obtained by increasing the upper lip camber. As

the maximum lift characteristics of inlets 1 through 3 were unsatisfactory, the camber of the upper lip was increased by reducing the lip extension to approximately 1.6 inches and by dropping the upper lip so that its nose radius was nearly on the chord line, thereby decreasing the inlet height 41 percent below that for inlet 1. (See fig. 3.) The lip stagger was further increased to 31°, which reference 1 indicates is approximately the maximum stagger that can be used without penalizing the pressure recoveries in the inlet at low values of lift coefficient.

The maximum lift coefficients for the model with inlet 4 installed (fig. 10(e)), were 1.07 and 1.76 with the 0° and 65° wing flaps, respectively, at a flow ratio of 0.14. These values are each slightly higher than corresponding values for inlet 1 but are still considerably lower than those for the basic wing. The section drag coefficients for this configuration (fig. 12) were of

the order of 0.0081 as compared to 0.0077 for the basic wing and were the lowest of any inlet configuration tested. The critical speeds for this inlet (figs. 14, 15, and 16) were higher than those for the other inlets tested over the more important portion of the operating range.

Inlet number 5. In inlet number 5 (fig. 3) the previously employed lip stagger angle of 31° was retained but the lip extension was reduced from 1.4 inches to 0.9 inch. The inlet height was 40 percent below that of inlet 1 to give inlet-velocity ratios approximately equal to those for inlet 4, and the center of the nose radius of the upper lip was located on the chord line to further increase the camber. To obtain as high a critical speed as possible with the added camber, the well established high-critical-speed inlet ordinates of reference 7 were applied to the upper lip by using the chord line of the airfoil as the reference line and the distance from the nose of the lip to the point of maximum airfoil thickness as the length of the section. Except for a greater ratio of inlet height to maximum wing thickness, this inlet configuration closely resembled the best inlets reported in reference 1.

The maximum lift coefficients for the model with inlet 5 installed and with propellers removed, figures 11(a) and 11(c) are compared in the following table with corresponding data for the basic model and for the model with inlet 1 installed:

Inlet	გ (deg)	Rt FtV <sub>0</sub>	$\frac{v_i}{v_o}$	C <sub>L</sub> max
Basic nose No. 1 No. 5	0	0.133 .140	0.493	1.20 1.05 1.21
Basic nose No. 1 No. 5	65	.138 .158	•503 •990	2.01 1.74 1.87

The maximum lift coefficient for the model with inlet 5 installed was slightly higher than that for the basic model for the 0 wing flap condition, but was still 0.14 less than that for the basic model with 65° wing flaps. A similar increase in C for 0° least

flap deflection, and decrease with 65° flap deflection with an inlet installed from that of the basic airfoil is presented in reference 1. The maximum lift coefficients for inlet 5, however, were considerably higher than those measured for the original inlet.

as for the basic airfoil sections.

The section drag coefficients measured for inlet 5 (fig. 12) varied from 0.0087 to 0.0096 as compared with 0.0077 for the basic wing and, although higher than those for inlet 4, were much lower than those for inlet 1.

The critical speeds for inlet 5(figs. 14, 15, and 16) were consistently higher than those for inlet 1 but in general were lower than those for inlet 4, the highest critical-speed configuration tested. For a typical high-speed, high-altitude flight condition at  $C_L = 0.40$  and  $\frac{Q_t}{F_t V_0} = 0.096$  (fig. 16) the predicted critical Mach number for this inlet was about 0.64 compared to 0.59 for the original inlet, 0.69 for inlet 4, and a desired value of 0.73 specified for the airplane. The predicted critical Mach number for the basic wing section ( $C_L \approx 0.40$ ) as obtained from tests in the Langley two-dimensional low-turbulence tunnels, has been shown to be only 0.64. Inlet 5, therefore, appears to meet the airplane specifications provided that the margin between the critical Mach number and the Mach number at which abrupt drag increases occur is the same for the inlet section

Total-pressure surveys at the measuring station in the internal ducting of inlet 5 are shown for high-speed and climb flight conditions (propeller removed) in figures 17 and 18, respectively. Attention is again called to the discontinuities in the internal lines of this inlet as shown in figures 3 and 4. The position of these surface discontinuities are shown by dotted lines on the cross-sectional views of the ducts in figures 17 and 18 to show that total-pressure measurements behind these ledges should not be taken as true indications of the total-pressure recovery: in most cases these tubes appeared to measure the static pressure of the stream at this station. Total-pressure recoveries were relatively high over most of the duct areas for the high-speed configuration (fig. 17); but excessive losses still occurred in the oil-cooler ducts in the climb configuration (fig. 18) because of the abrupt 90° expanding bend. For the climb condition, regions of low totalpressure recovery are noted also at the inboard sides of both parts of the inboard intercooler duct; these losses were probably caused by separation of the flow from the adjacent vanes. As there was no apparent means of obtaining satisfactory pressure recoveries at the oil cooler with the present duct arrangement, it is suggested that the oil-cooler cooling air be inducted through some source other than the wing inlet. It is apparent that further study is necessary

on the problem of designing vanes for inlets of this type when vanes appear to be necessary from strength considerations.

Lines of constant total-pressure recoveries at the measuring stations of inlet 5 are shown in figure 19(b) as a function of flow coefficient and lift coefficient. The higher desired rates of flow through the oil cooler ducts could not be obtained because of excessive duct losses as was the case with all other inlets. The total-pressure recoveries in both carburetor ducts and at the outboard intercooler duct were of the same order of magnitude as those for inlet 1 except in the climb range where some improvement was realized with inlet 5.

Inlet number 6 - Inlet number 6 was designed for an alternate longer-range version of the airplane with additional fuel tanks between the nacelles aft of the front wing spar. This installation involved the elimination of the intercooler and carburetor ducts aft of the front spar and the relocation of these ducts to enter the nacelle in front of the spar. To allow for the relocation of the ducting, the top lip was extended about 1.86 inches forward of the top lip for inlet 5. Because smaller flow quantities were required, it was possible to reduce the inlet height approximately 15 percent below that of inlet 5 by raising the lower lip. In other respects the design of the inlet (fig. 3) was generally similar to that of inlet 5. For these tests, the ducting forward of the spar was not simulated; the oil-cooler duct entrances to the nacelle were sealed off and the internal lines were faired to the measuring stations in the carburetor and intercooler ducts as shown in figure 5.

The maximum lift coefficients for the model with inlet 6 installed (figs. 10(f) and 10(g)) are compared in the following table with corresponding values for the basic nose and inlet number 5:

Inlet	δ (deg)	Qt FtVo	V <sub>i</sub> V <sub>o</sub>	C <sub>L</sub> max
Basic nose No. 5 No. 6	0	0.140	0.877	1.20 1.21 1.22
Basic nose No. 5 No. 6	65	.158 .168	.990	2.01 1.87 2.00

The maximum lift coefficients with inlet number 6 installed were higher than those for inlet 5 and were approximately equal to those for the basic nose installation. The section drag coefficients for inlet 6 (fig. 12) were higher than those for inlet 5, however, possible because of unavoidable roughness on the large areas of the modeling clay fairing required with this inlet. Surface-pressure distributions (fig. 14) indicate that the friction drag for inlet 6 should not be appreciably higher than that for inlet 5. The predicted critical Mach numbers for inlet 6 (figs. 15 and 16) were approximately equal to those for inlet 5.

Representative pressure surveys in the internal flow for inlet 6 are compared in figures 17 and 18 with those for inlets 1 and 5. The total-pressure recoveries for inlet 6 were higher than those for inlet 5, and in the climb condition there was no indication of flow separation from either the lower lip of the inlet or from the divider vanes. (See fig. 18.) Average total-pressure recoveries at the measuring stations in the ducting of inlet 6 are spotted on the pressure recovery charts for inlets 1 and 5 in figure 19. These recoveries appeared to be somewhat higher than those for the other inlets in the intercooler ducts and of the same magnitude as those for the other inlets in the carburetor ducts. The improved total-pressure recoveries in the inboard intercooler duct of inlet 6 are attributed to the elimination of the inboard oil-cooler duct with its divider vane.

Effect of end plate. An indication of the effectiveness of the end plate is afforded by comparisons of the lift curves for inlet 6 for the end-plate-installed and end-plate-removed conditions. At a flow coefficient of 0.175, removal of the end plate reduced the maximum lift coefficient with 0° wing flaps (fig. 10(f)) from 1.22 to 1.15, but did not cause any large change in the slope of the lift curves. With 65° wing flaps, (fig. 10(g)) removal of the end plate reduced the maximum lift coefficient from 2.00 to 1.70 and also reduced the slope of lift curve.

Effect of propeller operation. Supplemental tests were conducted with the number 5 inlet installed to study the effects of propeller operation on the aerodynamic characteristics of the model. In addition to tests with right-hand propellers as used on the airplane, tests were conducted with left-hand propellers to simulate the slipstream configuration for the right wing of the airplane.

The effects of propeller operation on the lift characteristics of the model are presented in figure 11. The maximum lift

coefficients for the right-hand propellers installation are compared with propeller-removed data in the following table:

		The same and the s	TO AND THE REST OF THE PARTY OF	******************
ర్ (deg)	Тc	F <sub>t</sub> v <sub>o</sub>	$\frac{v_i}{v_o}$	C <sub>L</sub> max
00	Props. off 0 .15	0.140 .145 (approx.) .145 (approx.)	0.877 .906 (approx.) .906 (approx.)	1.21 1.25 1.50
65°	Props. off 0.15	.158 .186 (approx.)	.990 1.164 (approx.)	1

Increases in thrust coefficient gave increases in C for

the left-hand propeller installation but the quantitative values obtained were not as great as those for the right-hand propeller installation.

The total-pressure recoveries at the measuring station in the inboard intercooler duct of inlet 5 are presented in figure 20 as a function of flow coefficient and lift coefficient for both right- and left-hand modes of propeller rotation. These total pressures were higher than those for the propeller-removed condition (fig. 19(b)). In most cases, the increases were a large percentage of the theoretical total-pressure rise through

a uniformally loaded propeller disk  $\left(\frac{8}{\pi}T_{c}\right)$ . These theoretical total-pressure rises are as follows:

Tc	н - н <sub>о</sub>
0.005	0.01
.035	.09
.090	.23
.150	.38

#### SUMMARY OF RESULTS

The more important results of this investigation are summarized as follows:

- l. The original inlet was found to decrease the maximum lift coefficients and to have critical Mach numbers below those of the wing with the basic nose installed.
- 2. The total-pressure recovery in the oil-cooler ducts was poor regardless of the inlet installation. As the sharp expanding bend in this duct cannot be avoided, it is recommended that the oil-cooler air be induced through the cowling or from some source other than the subject wing inlet.
- 3. Two inlets (nos. 5 and 6) were developed which should be satisfactory for the airplane. The maximum lift coefficients for the model with inlets 5 and 6 installed were about 1.21  $\left(\frac{Q_t}{F_t V_0} = 0.140\right)$  and 1.22  $\left(\frac{Q_t}{F_t V_0} = 0.129\right)$ , respectively, with 0° wing flaps

and 1.22  $\left(\frac{Q_t}{F_t V_o} = 0.129\right)$ , respectively, with 0° wing flaps and 1.87  $\left(\frac{Q_t}{F_t V_o} = 0.158\right)$  and 2.00  $\left(\frac{Q_t}{F_t V_o} = 0.168\right)$ , respectively,

with 65 wing flaps compared to corresponding values of 1.20 and 2.01 for the model equipped with the faired basic nose.

- 4. The predicted critical Mach numbers for inlets 5 and 6 for the critical military power high-speed condition for an altitude of 40,000 feet were 0.63 and 0.64, respectively, as compared with 0.64 for the thickest section of the basic wing.
- 5. Propeller operation (either right- or left-hand) caused appreciable increases in maximum lift coefficients and in the total pressures in the ducting.

Langley Memorial Aeronautical Laboratory
National Advisory Committee for Aeronautics
Langley Field, Va.

#### REFERENCES

- Racisz, Stanley F .: Development of Wing Inlets, NACA ACR No. L6318, 1946.
- Corson, Blake W., Jr.: The Belt Method for Measuring Pressure Distribution. NACA RB, Feb. 1943.
- 3. Alexander, S.R., and Sivells, James C.: Tests of a 1/14-Scale Powered Model of the XB-36 Airplane in the Langley 19-Foot Pressure Tunnel. I - Stalling Characteristics and Aileron Effectiveness of Several Wing and Flap Arrangements. NACA MR No. L5B23, 1945.
- 4. Sivells, James C., and Deters, Owen J.: Jet-Boundary and Plan-Form Conrections for Partial-Span Models with Reflection Flane, End Plate, or No End Plate in a Closed Circular Wind Tunnel. NACA TN No. 1077, 1946.
- 5. Silverstein, A., and Katzoff, S.: A Simplified Method for Determining Wing Profile Drag in Flight. Jour. Aero. Sci., vol. 7, no. 7, May 1940, pp. 295-301.
- 6. von Karman, Th.: Compressibility Effects in Aerodynamics. Jour. Aero. Sci., vol. 8, no. 9, July 1941, pp. 337-356.
- 7. Baals, Donald D., Smith, Norman F., and Wright, John B.: The Development and Application of High-Critical-Speed Nose Inlots. NACA ACR No. L5F30a, 1945.

and the season of the experimental and the contract of the season of the season of the season of the season of

tera a mentingga ta pada terapa mangan kangan pada terapa pada terapa terapa terapa terapa terapa terapa terap

# TABLE I.- ORDINATES FOR THE NUMBER 1 INLET (See figure 3 for symbol definitions) All ordinates in inches

		Station nord = 44	55.125	1	Wing Station 90.125  [Basic chord = 39.388 in.]						
x	Upper	Lip	Lower Lip			Upper	Lip	Lower Lip			
^	Yı	Y <sub>2</sub>	Y <sub>3</sub>	Y <sub>4</sub>	Х	Yı	Y2	¥ <sub>3</sub>	Y <sub>4</sub>		
0.561 1.121 2.242 3.363 4.483 6.725 7.599 7.695 8.130 8.148	1.130 1.562 2.168 2.621 2.987 3.547	0.231, .337, .615*	-1.666 -1.649*	-2.690 -2.816 -2.894 -2.989  -3.028**	0.492 .985 1.970 2.954 3.939 5.908 6.780 6.876 7.300 7.345	0.962 1.340 1.867 2.259 2.576 3.063	0.213 .300 .548*	-1.442 -1.474*	-2.278 -2.362 -2.416 -2.490 -2.520**		
Leadin radius	g-edge	0.464	0.3	17		0.382		0.2	60		
Leadin radius chord	off	.721	-2.1	63	.616			-1.842			
Leading-edge radius aft of O-percent chord		.800	1.598		. 677			1.347			

NATIONAL ADVISORY
COMMITTEE FOR AERONAUTICS

<sup>#</sup> Fairs to next ordinate with straight line

<sup>\*\*</sup> Fairs with airfoil contour

TABLE II.- ORDINATES FOR THE NUMBER 2 INLET
(See figure 3 for symbol definitions)
All ordinates in inches

		_		ation 5	_		Model Wing Station 90.125  Basic chord = 39.388 in.						
-		Basic chord = 44.833 in.						[20010 01014 3 00.000 111.]					
	U	Upper Lip Low				ip Upper Lip			р		Lower Li	р	
	х	Yı	Y2	х	¥3	Y4	Х	Yı	Y2	х	Ч3	Y4	
	0.229 .237 .280 .347 .380 .430 .500 .750 1.000 1.750 2.250 2.750 3.250 3.750 4.250 4.750 5.250 6.750 6.250 6.750 7.250 7.250 8.141	0.989  1.149 1.254 1.437 1.577 1.737 1.981 2.194 2.385 2.566 2.735 2.889 3.035 3.167 3.291 3.408 3.522 3.631  3.735 3.818*	0.549 -509 .469 -429 .402 .342 .319 .313 .332 .375 .437 .513 .596 .684 .782 .883 .989 1.102 1.228 1.369 1.484	1.450 1.550 1.650 1.750 2.000 2.250 3.250 3.250 4.250 4.750 5.250 5.750 6.250 6.750 7.250 7.695 7.750 8.130	-1.768 -1.632 -1.595 -1.595 -1.530 -1.483 -1.416 -1.370 -1.337 -1.312 -1.295 -1.281 -1.270 -1.265 -1.264 -1.264	-1.977 -2.055 -2.102 -2.151 -2.257 -2.343 -2.492 -2.608 -2.702 -2.783 -2.843 -2.890 -2.926 -2.955 -2.980 -3.0013.019 -3.028*	0.185 .205 .220 .230 .250 .350 .450 .550 .750 1.000 1.250 2.750 3.250 3.750 4.250 5.250 6.250 6.750 6.750 6.750 7.250 7.345	U.809 .848 .873 .888 .916 1.029 1.120 1.198 1.333 1.477 1.603 1.824 2.024 2.201 2.356 2.498 2.634 2.757 2.876 2.986 3.086	0.457 .414 .384 .338 .329 .355 .405 .473 .550 .641 .746 .870 1.008 1.162 1.335	1.289 1.290 1.330 1.333 1.360 1.383 1.450 1.500 2.750 2.250 2.750 3.250 3.750 4.250 4.250 6.250 6.250 6.876 7.300	-1.131 -1.391 -1.371 -1.331 -1.303 -1.229 -1.181 -1.143 -1.095 -1.063 -1.050 -1.052 -1.063 -1.116 -1.148 -1.1187 -1.198	-1.558 -1.629 -1.671 -1.770 -1.737 -1.844 -1.941 -2.006 -2.129 -2.233 -2.297 -2.352 -2.395 -2.457 -2.481 -2.501 -2.520*	
	Leadin radius	g-edge	0.233		0.153			0.238	<u> </u>		0.125		
	radius	Leading-edge radius off chord line			-1.866			0.709			-1.511		
	Leading-edge radius aft of 0-percent chord 0.384		1.560			0.401			1.385				

NATIONAL ADVISORY
COMMITTEE FOR AERONAUTICS

Fairs with airfoil contour

## TABLE III.- ORDINATES FOR THE NUMBER 3 INLET (See figure 3 for symbol definitions) All ordinates in inches

		_	tation 5	_			_		= 39.388	_		
2	Upper I	ip		Lower Li	р	Upper Lip			Lower Lip			
х	Yı	Y2	х	Y3	Y <sub>4</sub>	х	Yı	Y2	х	Y3	Y4	
-3.090 -3.067 -3.045 -3.023 -3.000 -2.870 -2.750 -2.500 -2.250 -1.500 -1.500 -1.500 -1.500 2.500 3.500 4.500 4.500 5.500 6.500 7.500 7.599 7.880  Leadin	0.597 .648 .695 .738 .767  1.017 1.198 1.352 1.490 1.619 1.735 1.849 1.955 2.145 2.318 2.476 2.318 2.476 2.627 2.762 2.900 3.010 3.120	0.200 149 .092 .072 .069 .072 .084 .105 .129 .189 .253 .323 .323 .323 .323 .323 .323 .323	-1.989 -1.944 -1.899 -1.854 -1.724 -1.630 -1.500 -1.250 -1.000 -1.500 0.500 1.500 2.060 2.500 3.500 4.000 4.500 5.500 6.500 7.000 7.500 7.695 8.130	-1.652 -1.615 -1.584 -1.561 -1.504 -1.471 -1.435 -1.390 -1.357 -1.311 -1.280 -1.262 -1.252 -1.244 -1.241 -1.241 -1.241 -1.243 -1.244 -1.245 -1.256 -1.266 -1.264 -1.264	-1.906 -1.943 -1.973 -1.998 -2.061 -2.101 -2.152 -2.248 -2.330 -2.468 -2.573 -2.658 -2.727 -2.864 -2.922 -2.947 -2.965 -2.983 -2.997 -3.012 -3.027 -3.040 -3.0513.066	-2.859 -2.838 -2.818 -2.618 -2.518 -2.518 -2.318 -2.318 -2.318 -2.350 -2.000 -1.750 -1.500 -1.500 -1.500 0 5.500 1.500 2.500 3.500 4.500 5.500 5.500 6.780	0.575615.643 .756.847 .925.944 1.060 1.101 1.237 1.362 1.476 1.580 1.678 1.855 2.020 2.168 2.308 2.438 2.562 2.678 2.788 2.991 2.992 3.088 3.185 3.274 3.361 3.440 3.513	0.184 .141 .1090 .075 .068 .055 .056 .067 .085 .107 .163 .234 .305 .389 .475 .567 .970 1.075 1.177 1.283 1.386 1.491 1.551	-1.959 -1.956 -1.917 -1.914 -1.887 -1.864 -1.1.500 -1.250 -1.000750500 0 .500 1.000 2.000 2.500 3.500 4.500 5.500 6.500 6.500 7.000 6.876	-1.461 -1.421 -1.401 -1.333 -1.258 -1.213 -1.185 -1.156 -1.137 -1.109 -1.084 -1.0094 -1.100 -1.112 -1.121 -1.143 -1.155 -1.178 -1.190 -1.198	-1.66 -1.76 -1.76 -1.76 -1.86 -1.98 -1.90 -2.09 -2.14 -2.23 -2.35 -2.35 -2.39 -2.44 -2.46 -2.49 -2.50 -2.51 -2.52 -2.53 -2.53	
Leading	radius 0.233  Leading-edge radius off chord line 0.478			-1.780			0.436			-1.541		
Leading-edge radius aft of O-percent chord		-2.866	-1.898			-2.667			-1.859  NATIONAL ADVISORY COMMITTEE FOR AERONAUTICS			

### TABLE IV.- ORDINATES FOR THE NUMBER 4 INLET (See figure 3 for symbol definitions)

All ordinates in inches

		Wing St		_	,			wing St		_	
	Upper Lip Lower Lip					U	pper Lip		Lower Lip		
х	Yı	Y2	х	Y3	Y <sub>4</sub>	х	Y <sub>1</sub>	Y <sub>2</sub>	х	Y <sub>3</sub>	• Y4
-1.408 -1.390 -1.367 -1.345 -1.300 -1.255 -1.210 -1.166 -1.121 -1.031897785672560448224 0 0 448 .897 1.793 2.242 2.3138 3.587 4.035 4.483 4.932 5.828 6.277 7.300 7.605 7.622 8.070 8.141	0.247 .354 .420 .460 .529 .587 .641 .726 .811 .993 1.075 1.143 1.341 1.465 1.682 1.879 2.055 2.215 2.368 2.514 2.652 2.785 2.912 3.349 3.450 3.143 3.250 3.349 3.450 3.551 3.641 	0.140 .108 .081 .040 .008 - 013 - 040 - 058 - 093 - 130 - 134 - 130 - 116 - 088 - 039 .030 .105 .180 .260 .332*	-0.215202179134090045 0 0.045 0.090134179224336448672877345179324269013835870354.833802751732404006226856006226856006226856708130	-1.770 -1.698 -1.645 -1.584 -1.540 -1.500 -1.471 -1.442 -1.3742 -1.354 -1.314 -1.275 -1.219 -1.166 -1.090 -1.030 -0.980945922923*	-1.89( -1.929 -1.982 -2./23 -2.058088 2.122 -2.143 -2.170 -2.264 -2.385 -2.450 -2.552 -2.633 -2.694 -2.793 -2.830 -2.830 -2.912 -2.954 -2.968 -2.912 -2.968 -3.003 -3.028**	-1.237 -1.221 -1.101 -1.182 -1.142 -1.103 -1.063 -1.0985906788689591492394197 0 394788182187 0 3941821	0.209 .293 .293 .503 .449 .503 .585 .624 .688 .908 .908 .1028 1.136 1.240 1.424 1.591 1.881 2.011 2.135 2.250 2.359 2.467 2.569 2.467 2.569 2.676 2.777 2.875 3.080 3.141 3.287 3.334***	0.122 .091 .068 .034 .006 015 035 049 106 114 099 106 117 114 099 010 .042 .108*	-0.189 -177 -158 -118 -079 -039 0 039 -079 -118 -158 -197 -295 -394 -591 -788 -1.82 -1.576 -1.969 -2.363 -2.757 -3.151 -3.939 -4.333 -4.727 -5.120 -5.514 -5.908 -6.906 -6.96 -6.96 -6.96 -6.96 -6.96 -6.96 -6.96 -6.96 -6.96	-1.501 -1.437 -1.395 -1.340 -1.300 -1.270 -1.224 -1.199 -1.181 -1.165 -1.149 -1.114 -1.034 -0.988920865820760760760760*	-1.602 -1.633 -1.680 -1.715 -1.745 -1.770 -1.878 -1.857 -1.878 -1.923 -1.960 -2.025 -2.080 -2.168 -2.235 -2.278 -2.380 -2.380 -2.420 -2.432 -2.450 -2.450 -2.450 -2.55082.5082.508

NATIONAL ADVISORY COMMITTEE FOR AERONAUTICS

<sup>\*</sup> Fairs to next ordinate with straight line

<sup>\*\*</sup> Fairs with airfoil contour

TABLE V.- ORDINATES FOR THE NUMBER 5 INLET
(See figure 3 for symbol definitions)

All ordinates in inches

	Г	l Wing St		7		Model Wing Station 90.125  [Basic chord = 39.388 in.]						
	Upper Lip Lower Lip						Upper Lip			Lower Lip	)	
х	Yı	Y2	Х	Y3	Y <sub>4</sub>	Х	Yı	Y <sub>2</sub>	Х	Y3	Y4	
-0.900	0.030	0.030	0.205	-1.820		-0.791	0	0	0.180	-1.543		
895	.092	024	.218	-1.748	-1.940	785	.085	033	.192	-1.482	-1.645	
890	.128	043	.241	-1.695	-1.979	780	.122	(48	.212	-1.437		
880	.172	076	.286	-1.634	-2.032	770	.162	075		-1.437	-1.678	
870	.208	095	.330	-1.590					.251		-1.723	
860	.238	115	.375	-1.550	-2.073	760	.190	088	.290	-1.348	-1.757	
840	. 283	138	.420	-1.521	-2.108	750	.222	103	.329	-1.314	-1.787	
820	.323	158	.465	-1.492	-2.172	740 730	.250	112	.369	-1.290	-1.813	
800	.364	172	.510	-1.492			.373	120	.409	-1.265	-1.841	
750	.444	202	.554	-1.444	-2.193	720	.293	128	.448	-1.246	-1.859	
.700	.512	223	.599	-1.422		640		143	.487	-1.224	-1.882	
600	.629	248	.644		-2.245		.414	179	.526	-1.206	-1.903	
.500		252	.756	-1.404	-2.270	- ,600	.462	195	.566	-1.190	-1.925	
.400	.823	250	.868	-1.364	-2.314	500	•567	215	.664	-1.156	-1.962	
200	.992	239	1.092	-1.269	-2.360	200	.668	216	.763	-1.123	-2.011	
0	1.142	223	1.317	-1.209	-2.435	0.200	.842	203	.959		-2.070	
.200	1.278	200	1.765	-1.140	-2.500	-	.990	190	1.157	-1.031	-2.125	
.400	1.402	172	2.213	-1.080	-2.602	.200	1.122	165	1.551	966	-2.212	
.600	1.525	138	2.662		-2.683	.400	1.245	138	1.944	916	-2.275	
.800	1.642	102		-1.032	-2.744	.600	1.362	105	2.339	875	-2.318	
1.000	1.747	068	2.690	-1.030 998	-2.748	.800	1.472	072	2.363	875	-2.319	
1.200	1.845	030*	3.587		-2.793	1.000	1.578	035	2.757	852	-2.350	
1.400	1.942	030"		982	-2.830	1.500	1.802	.059*	3.151	837	-2.380	
1.600	2.032		4.035	972"	-2.864	2.000	1.999		3.545	822	-2.401	
2.000	2.198		4.483		-2.888	2.500	2.162	F I I I I I	3.939	818*	-2.420	
2.500	2.198		4.932		-2.912	3.000	2.310		4.333		-2.432	
3.000	2.568		5.380		-2.935	3.500	2.448		4.727		-2.450	
3.500	2.732		5.828		-2.954	4.000	2.582		5.120		-2.461	
4.000	2.878		6.277		-2.969	5.000	2.842		5.514	200	-2.475	
4.500			6.725		-2.988	5.120	2.875		5.700	780		
5.550	3.017		7.173	1.055	-3.003	5.514	2.970	0.056	5.908		-2.490	
6.000	3.272		7.240	- '.955		5.700		0.852	6.302		-2.500	
6.500	3.387		7.400	962		5.800		.873	6.400	821		
	3.500		7.600	988		5.908	3.060		6.696		-2.508	
7.000	3.608	2 200	7.622		-3.017	6.200		.965	6.865	889		
7.300	7 704	1.100	7.685	-1.000		6.302	3.141		7.090		-2.519	
7.500	3.704	1.145	8.070		-3.023**	6.600		1.085	7.300		-2.520	
7.605		1.179				6.696	3.218					
8.000	3.798**					6.793	M.M.	1,156				
8.141						7.090	3.287**					

NATIONAL ADVISORY
COMMITTEE FOR AERONAUTICS

<sup>- \*</sup> Fairs to next ordinate with straight line

<sup>\*\*</sup> Fairs with airfoil contour

TABLE VI.- ORDINATES FOR THE NUMBER 6 INLET

(See figure 3 for symbol definitions)

All ordinates in inches

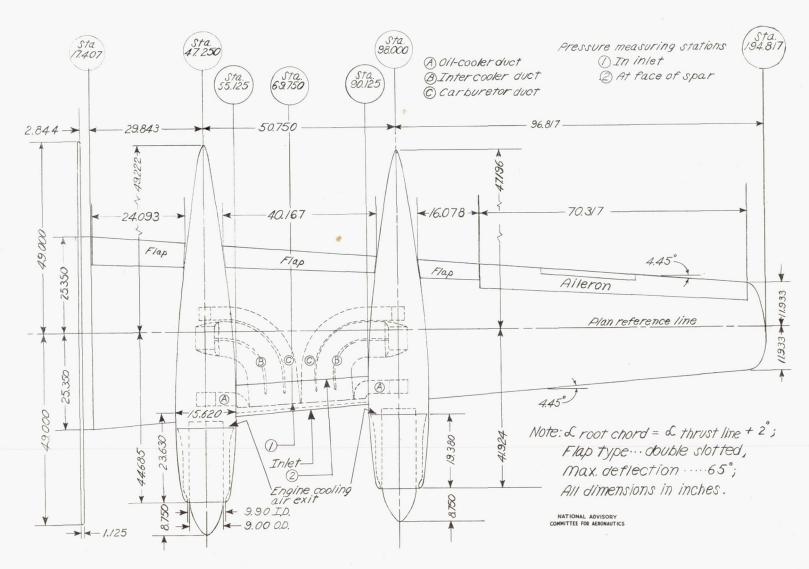
Model Wing Station 55.125 [Basic chord = 44.833 in.]					Model Wing Station 90.125 [Basic chord = 39.388 in.]				
	Upper Lip		Lower Lip			Upper Lip		Lower Lip	
х	Yı	Y2	Y <sub>3</sub>	Y <sub>4</sub>	х	Yı	Y-3	Y3	, Y <sub>4</sub>
-2.607 -2.477 -2.346 -1.953 -1.692 -1.168 -0.907 645 383 .925 2.233 4.850 7.467 10.083	0.431 .600 .733 1.066 1.250 1.419 1.571 1.775 1.849 1.974 2.495 2.913 3.541 3.964 4.268	-0.203 240 251 253 203 166 123 078 028 .020	-1.360 -1.241 -1.154 -1.084 -1.026 -0.835	-2.094 -2.205 -2.293 -2.360 -2.413 -2.581 -2.698 -2.876 -3.003 -3.083	-2.648 -2.526 -2.296 -2.061 -1.828 -1.358 -1.124 -0.989655 .517 1.689 4.033 6.378 8.722	0.330 .484 .610 .906 1.073 1.213 1.351 1.480 1.601 1.715 2.170 2.530 3.059 3.423 3.689	-0.156198215198160119074030014 .058	-1.123 -1.015 -0.935 874 823 670	-1.788 -1.854 -1.929 -1.979 -2.018 -2.129 -2.208 -2.334 -2.444 -2.514
Leading-edge radius		0.193	0.284		0.168		0.225		
Leading-edge radius off chord line		0	-1.734		0		-1.445		
Leading-edge radius aft of O-percent chord		-2.564	-1.452		-2.579  NATIONAL ADVISORY COMMITTEE FOR AERONAUTICS		-1.680		

TABLE VII
ORDINATES OF BASIC AIRFOIL SECTIONS

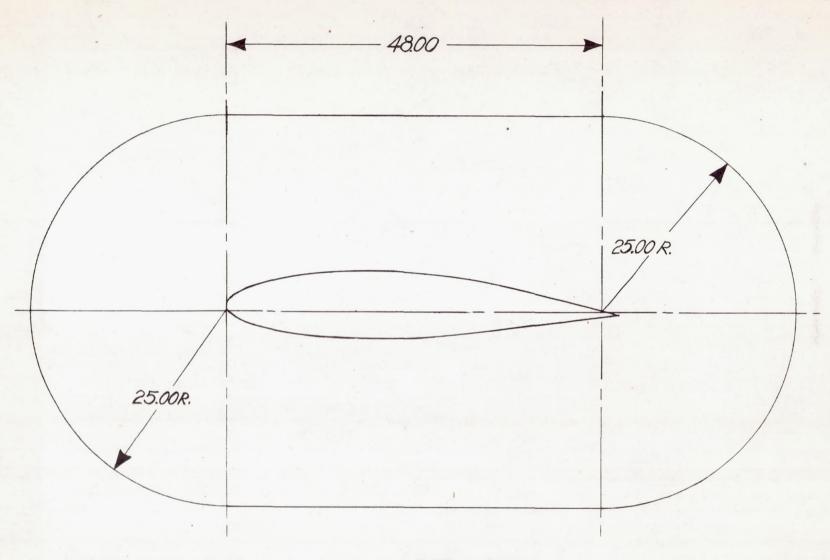
[Percent chord]

Station	Root section	(theoretical)	Tip section (theoretical)		
Station	Upper	Lower	Upper	Lower	
0.50 .75 1.25 2.50 5.00 7.50 10.00 15.00 20.00 25.00 30.00 35.00 40.00 45.00 50.00 65.00 70.00 75.00 80.00 85.00 90.00	1.759 2.084 2.609 3.595 4.967 5.993 6.813 8.089 9.023 9.707 10.183 10.482 10.609 10.569 10.365 9.991 9.447 8.742 7.882 6.869 5.733 4.494 3.141 1.663 .017	1.119 1.412 1.885 2.700 3.768 4.520 5.103 5.972 6.569 6.986 7.248 7.379 7.396 7.281 7.052 6.698 6.220 5.625 4.920 4.129 3.286 2.419 1.534 .677	1.408 1.667 2.095 2.924 4.120 5.019 5.771 6.930 7.818 8.467 8.938 9.247 9.399 9.242 8.429 7.736 6.886 5.879 4.791 3.638 2.436 1.245 .039	0.709 .888 1.175 1.646 2.231 2.609 2.869 3.459 3.606 3.654 3.654 3.654 3.654 3.654 3.653 2.896 2.653 2.398 2.101 1.765 1.402 1.002 .563 .039	
Leading-edge radius height	0.23	4	0.234		
Leading-edge radius	2.02	5	1.057		

NATIONAL ADVISORY COMMITTEE FOR AERONAUTICS.



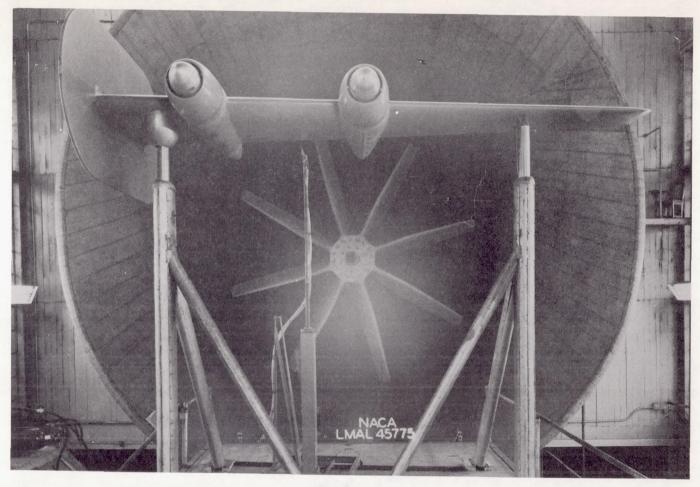
(a) General arrangement and principal dimensions. Figure 1.—The 1/4—scale semispan wing model used for tests.



(b) Details of end plate.

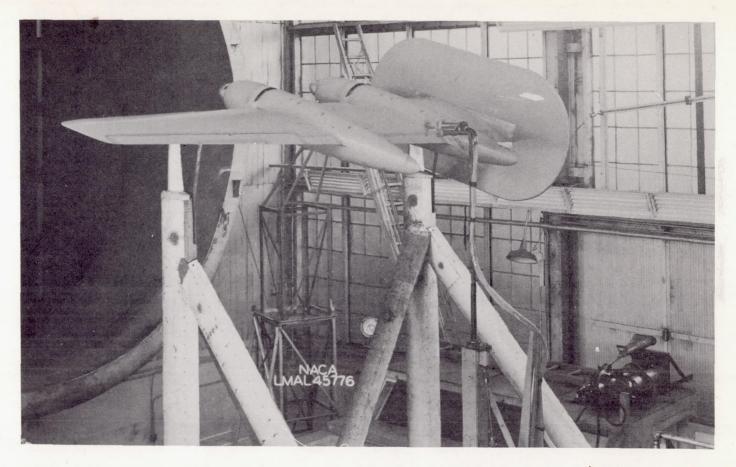
NATIONAL ADVISORY COMMITTEE FOR AERONAUTICS

Figure 1.- Continued.

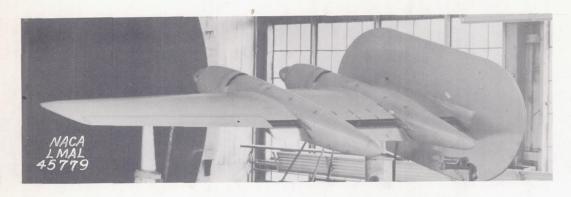


Photograph of model mounted in the Langley propeller-research tunnel; basic nose installed.

Figure 1.- Concluded.



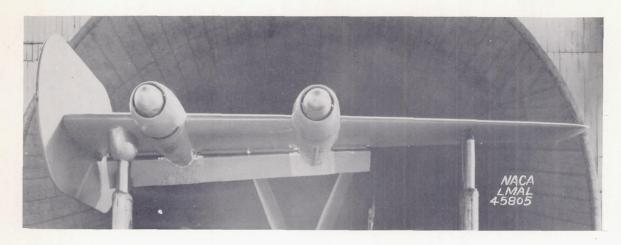
(a) Three-quarter rear view  $\delta = 0^{\circ}$ ; wake survey rake shown in position. Figure 2.- Photographs of model with various flap configurations installed.



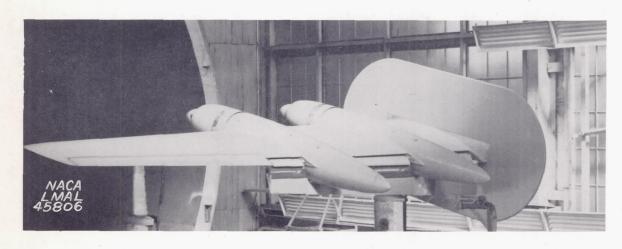
(b) Three-quarter rear view;  $\delta = 20^{\circ}$ .



(c) Three-quarter rear view;  $\delta = 65^{\circ}$ ; short cowling flaps installed on model. Figure 2.- Continued.



(d) Front view;  $\delta = 65^{\circ}$ ; continuous flap.



(e) Three-quarter rear view;  $\delta = 65^{\circ}$ ; continuous flap; long cowling flaps installed on model.

Figure 2.- Concluded.

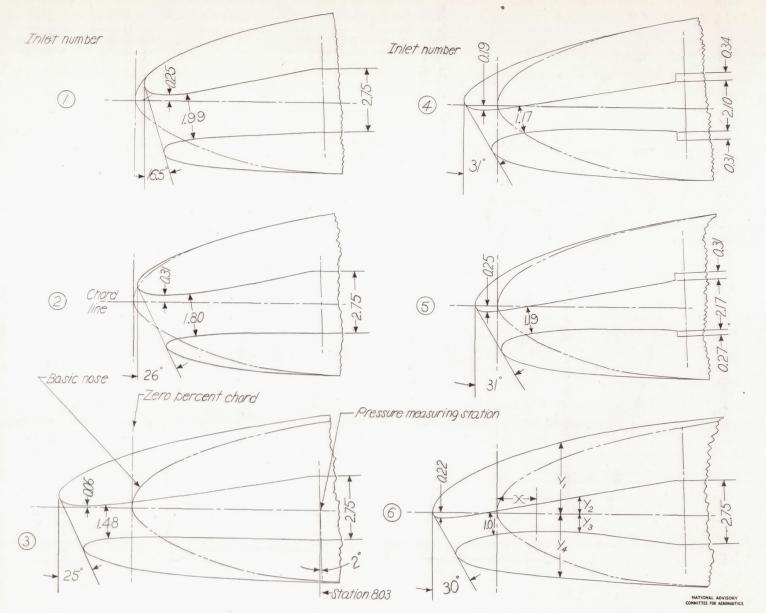


Figure 3.-Cross-sectional sketches of the several inlet lips compared with the basic airfoil contour at station 55.125.

See tables I through 6 for ordinates, all dimensions are in inches.

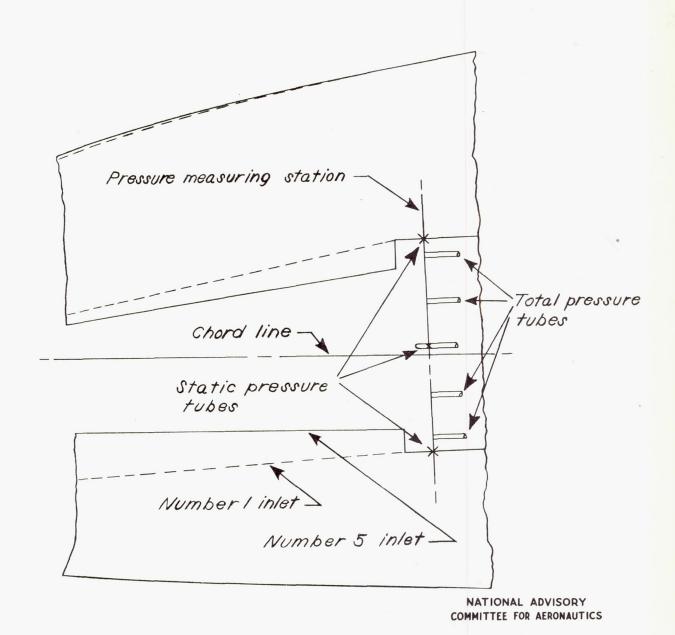


Figure 4.- Sketch showing position of discontinuity in diffuser fairing of inlet 5 relative to pressure tubes at measuring station.

Figure 5.- General view of model with right-hand propellers and inlet number 5 installed.

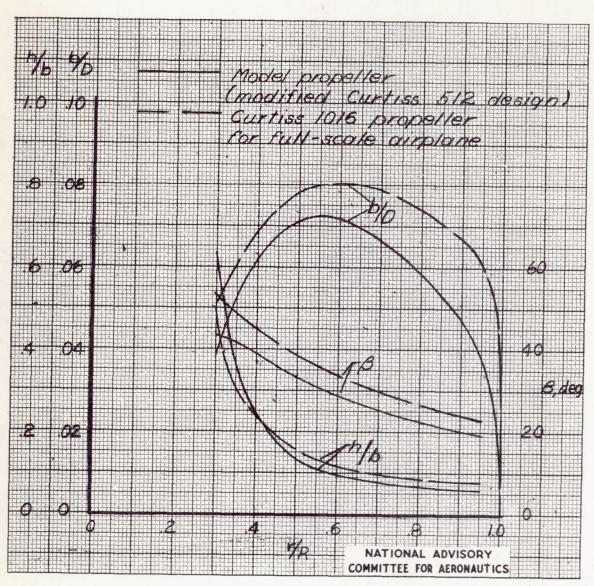


Figure 6.- Blade-form curves for model propeller and Curtiss 1016 propeller. D, diameter; R, radius to tip; r, station radius; b, section chord; h, section thickness;  $\beta$ , blade angle, degrees.

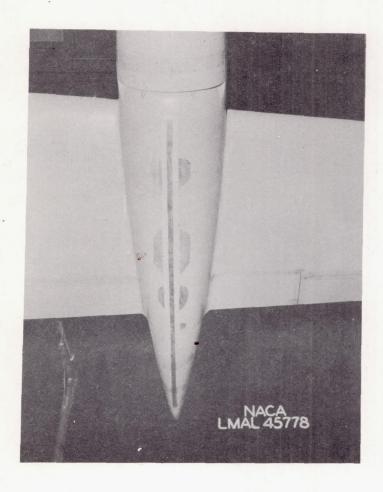


Figure 7.- Pressure belt installation on lower surface of outboard nacelle; duct exits sealed and faired.

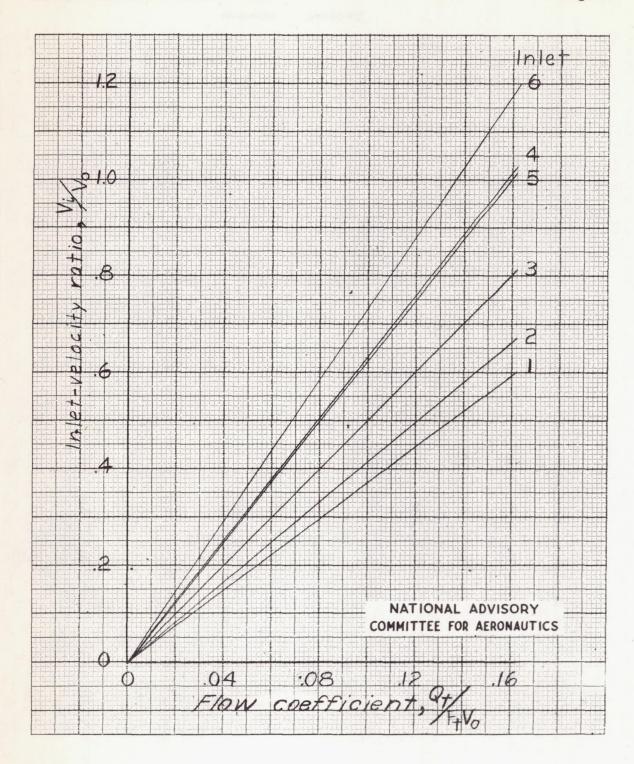


Figure 8.- Relationship of inlet-velocity ratio to total flow coefficient for the several inlets.

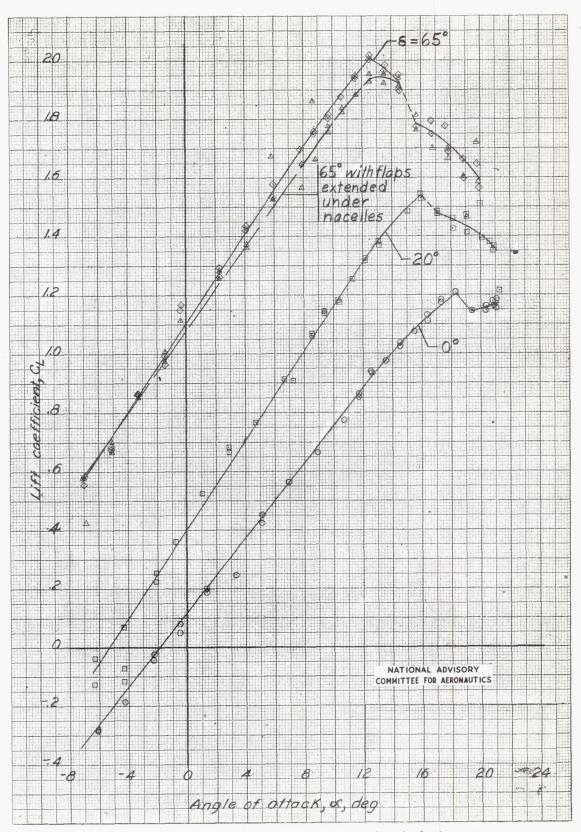
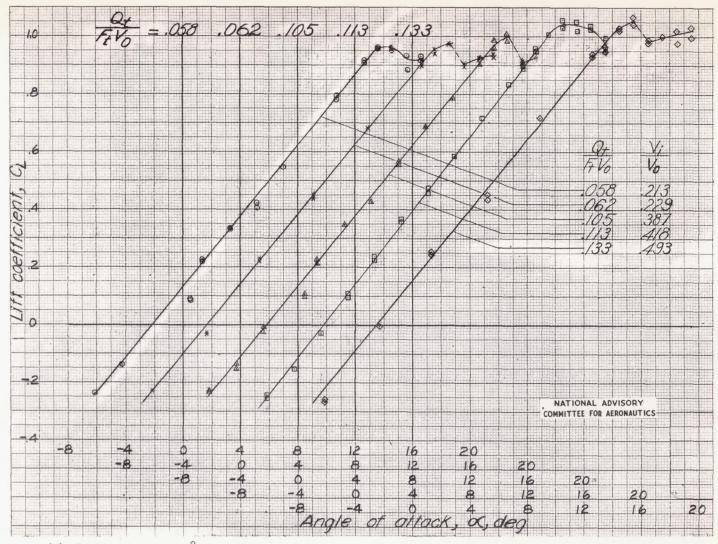
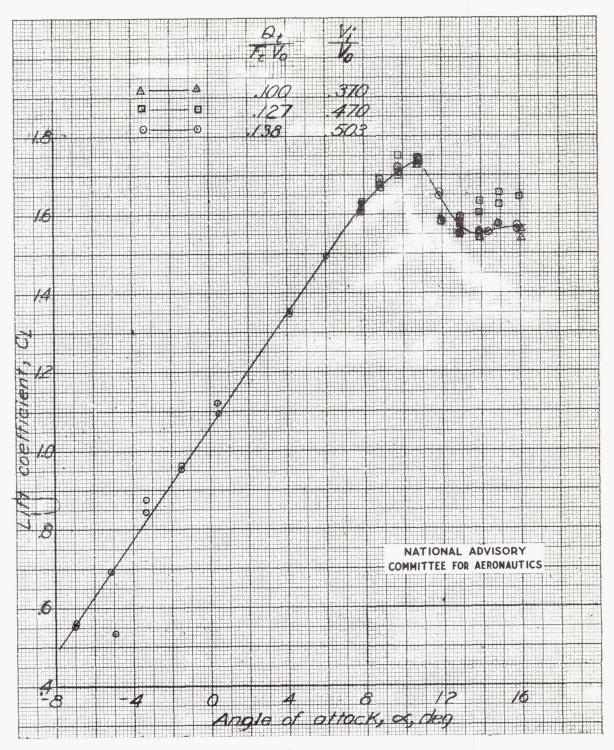


Figure 9.- Lift characteristics of the semispan wing model with the basic nose installed.



(a) Inlet number 1; 8, 0°.

Figure 10.- Lift characteristics of the semispan wing model with several of the inlets installed for several flow coefficients.



(b) Inlet number 1;  $\delta$ ,  $65^{\circ}$ .

Figure 10.- Continued

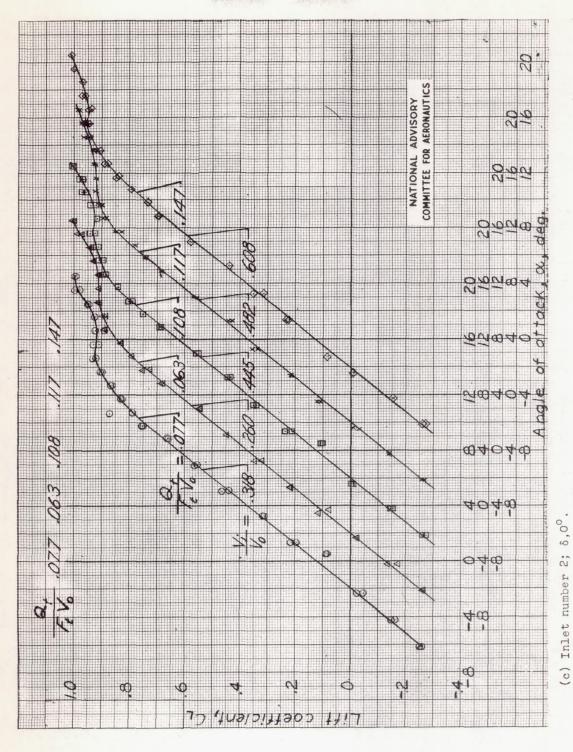
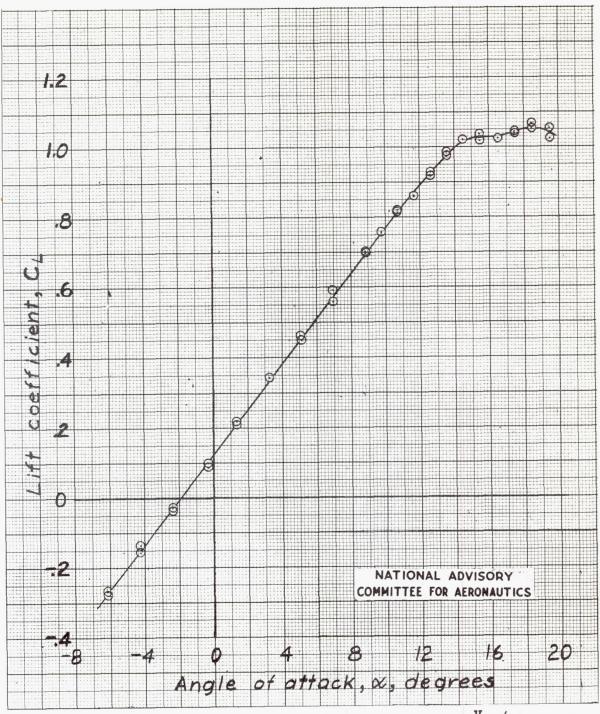


Figure 10.- Continued.



(d) Inlet number 3;  $\delta$ ,  $0^{\circ}$ ;  $Q_{t}/F_{t}V_{o}$ , 0.133;  $V_{1}/V_{o}$ , 0.667.

Figure 10.- Continued.

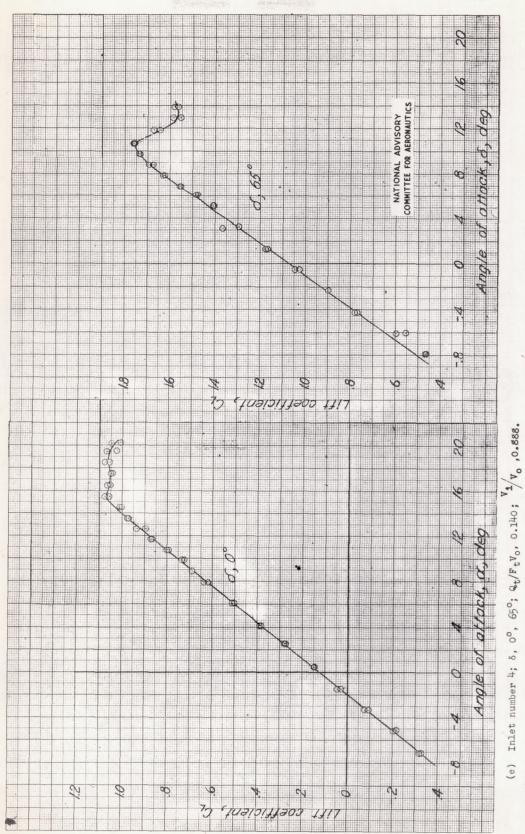
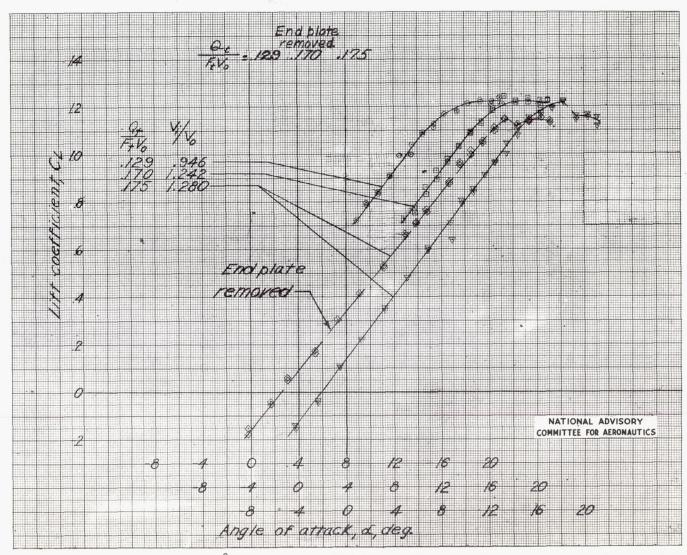
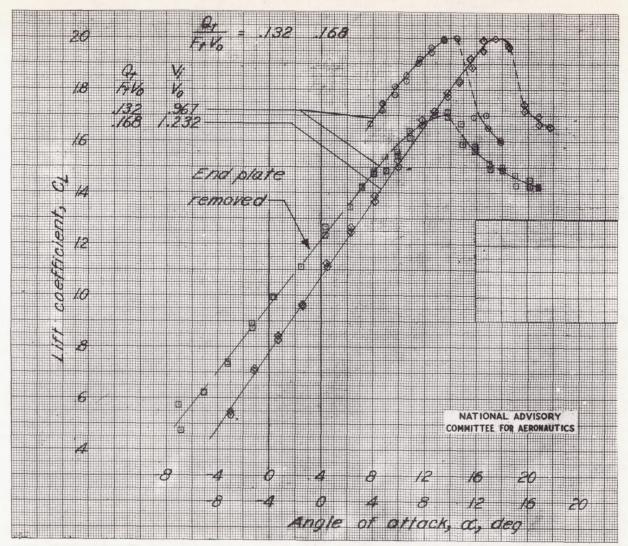


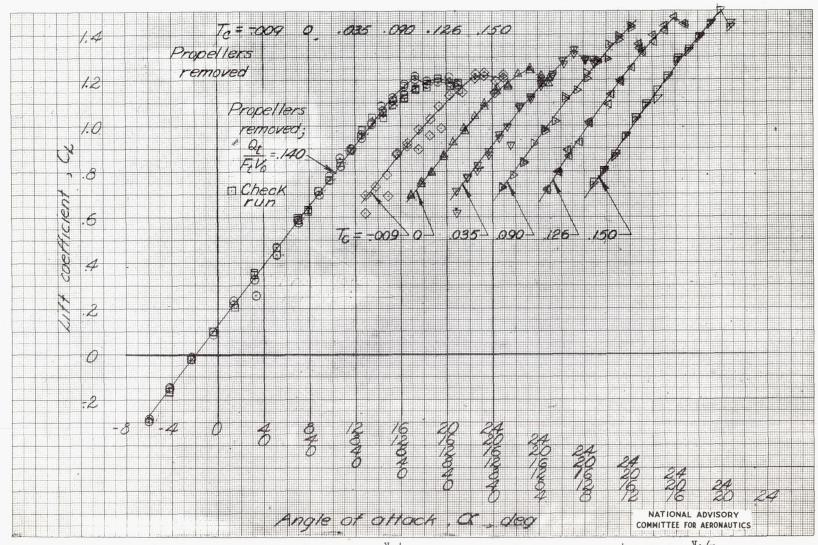
Figure 10.- Continued.



(f) Inlet number 6;  $\delta$ ,  $\delta$ , o end plate installed and end plate removed. Figure 10.- Continued.

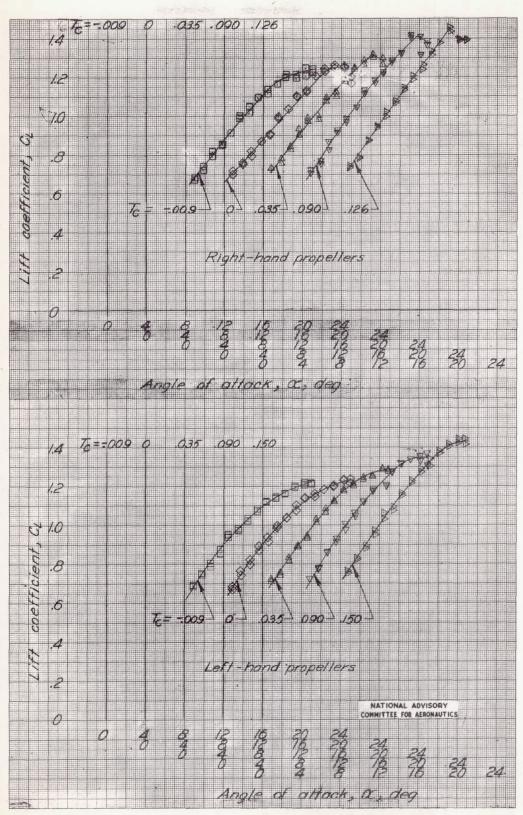


(g) Inlet number 6;  $\delta$ ,  $65^{\circ}$ ; end plate installed and end plate removed. Figure 10.- Concluded.

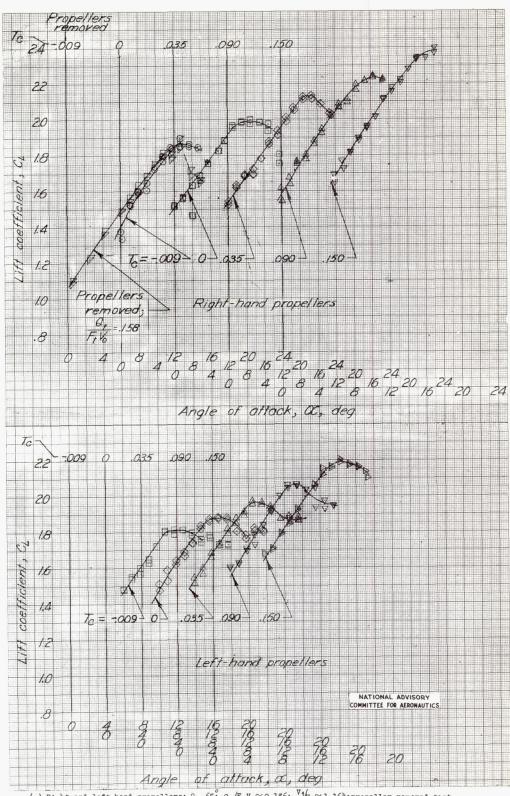


(a) Right-hand propellers;  $\delta$ ,  $0^{\circ}$ ;  $Q_t/F_tV_0\approx 0.145$ ;  $V_1/V_0\approx 0.906$ ; propeller removed test,  $Q_t/F_tV_0=0.140$ ;  $V_1/V_0=0.877$ .

Figure 11.- The effect of propeller operation on the wing lift characteristics with the number five inlet installed.

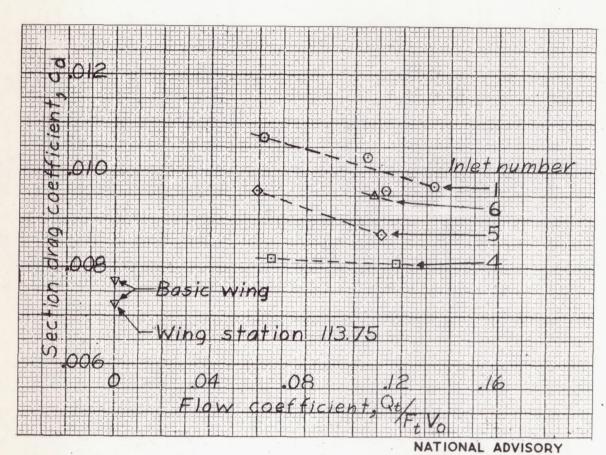


(b) Right-and left-hand propellers;  $\delta,~0^o;~Q_t/F_tV_0\approx 0.185; ^{V_1}/_{V_0}\approx 1.185.$  Figure ll.- Continued.



(c) Right-and left-hand propellers;  $\delta$ ,  $65^{\circ}$ ,  $Q_{\rm t}/F_{\rm t}v_{\rm o}\approx 0.186$ ;  $v_{\rm t}/v_{\rm o}\approx 1.164$ ; propeller removed test,  $Q_{\rm t}/F_{\rm t}v_{\rm o}\approx 0.158$ ;  $v_{\rm t}/v_{\rm o}\approx 0.990$ .

Figure 11.- Concluded.



COMMITTEE FOR AERONAUTICS

Figure 12.- Section drag coefficients for the several wing ducts at wing station 72.25, as a function of flow coefficient.  $\alpha$ , -2.4°.

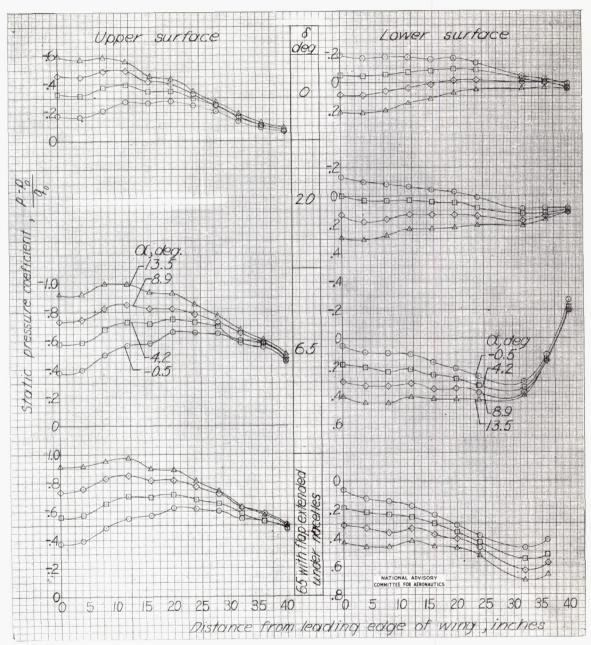


Figure 13.- Surface-pressure distributions on the upper and lower surfaces of the outboard nacelle; dect exits sealed and faired; basic nose installed.

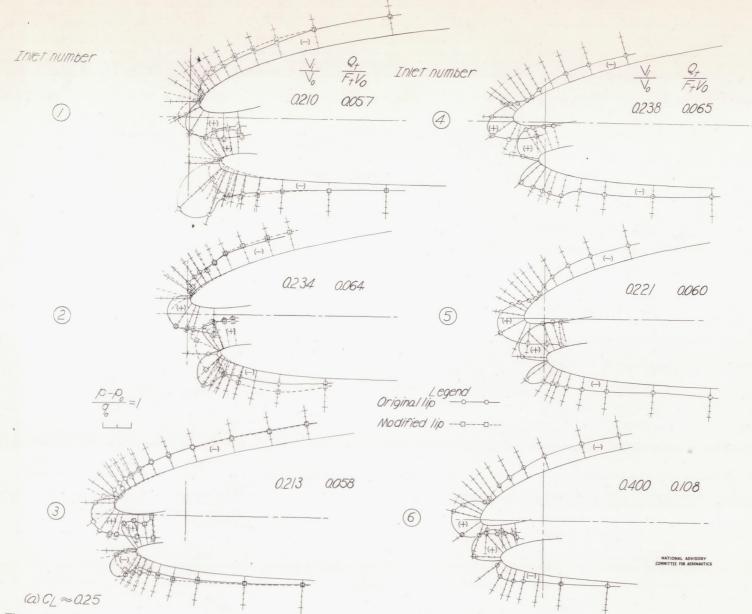
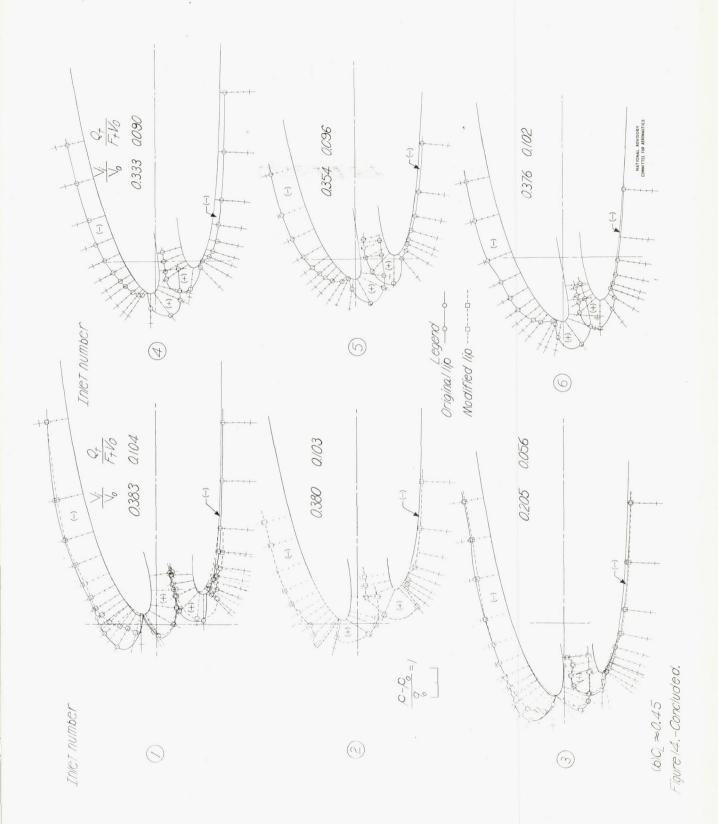


Figure 14. - Representative surface pressure distributions obtained with various inlets installed on the model. Wing station, 69.750.



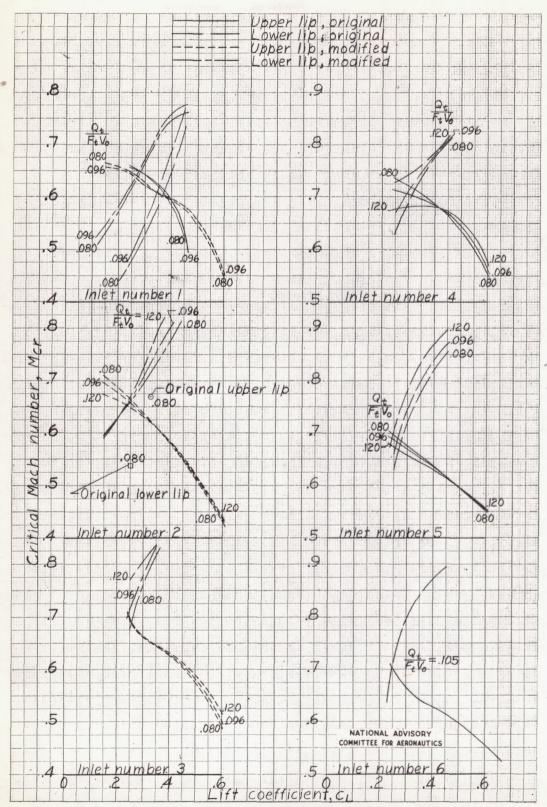


Figure 15.- Variation of the predicted critical Mach numbers with lift coefficient, for the upper and lower lips of the several inlet configurations.

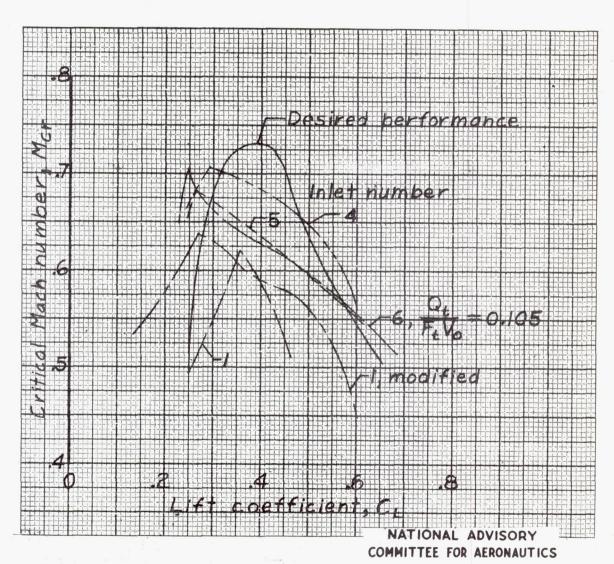
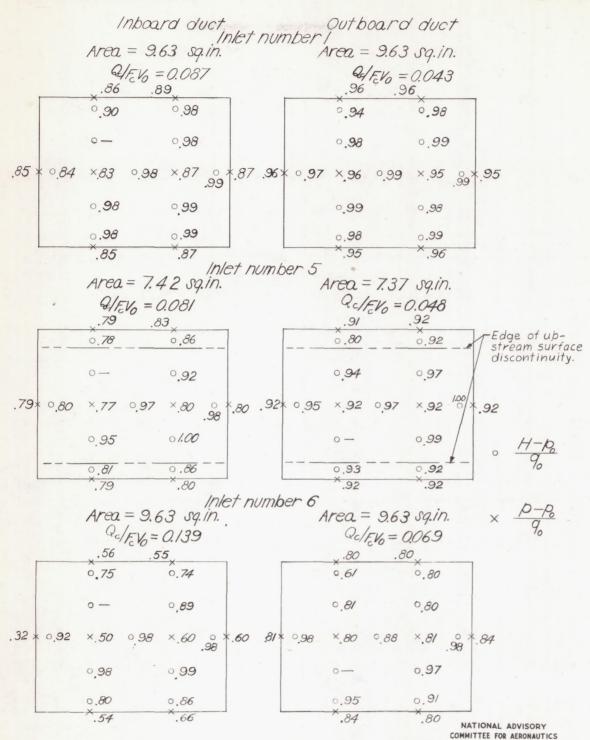


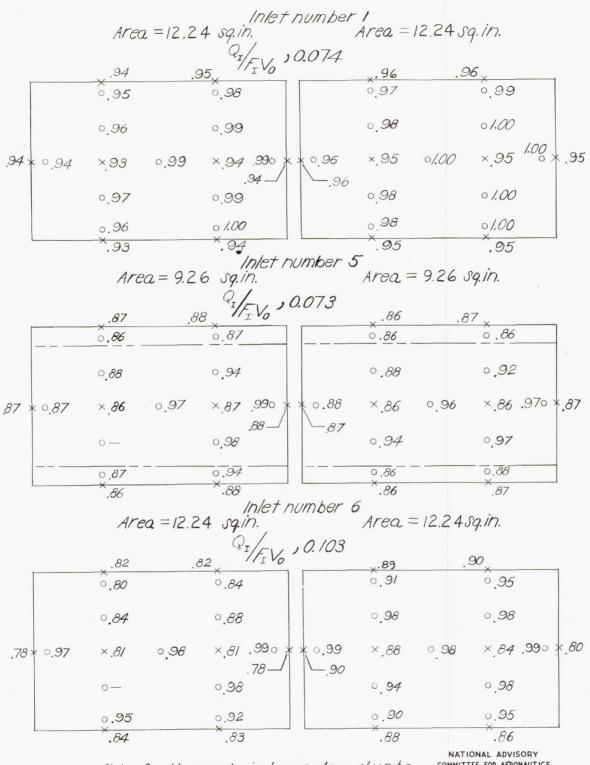
Figure 16.- Indicated critical Mach numbers for several inlet configurations as function of lift coefficient. Qt/FtVo = 0.096.



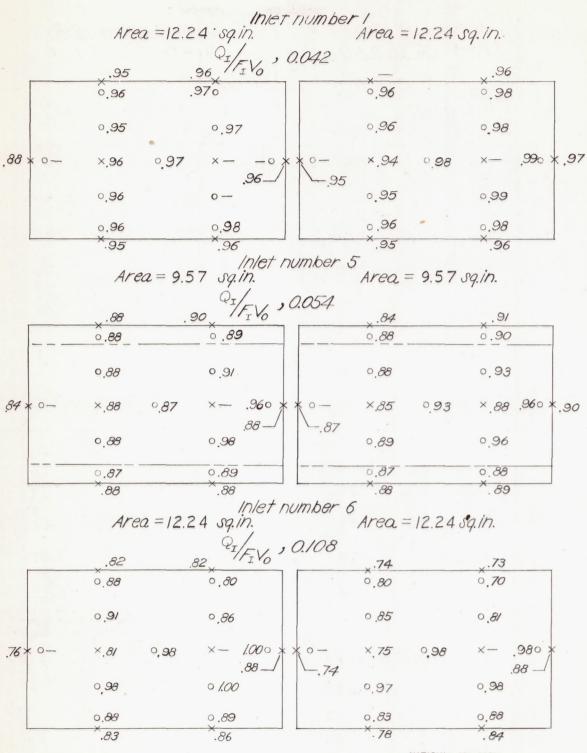
(a) Inboard and outboard carburefor ducts,

Figure 17. - Representative distributions of total

and static pressure coefficients at meas
uring stations in ducting for the pro
peller-removed high speed condition; C∠≈0.25.



(b) Outboard intercooler ducts. COMMITTEE FOR AERONAUTICS
Figure 17. - Continued.



(c) Inboard intercooler ducts.

Figure 17. - Continued.

NATIONAL ADVISORY COMMITTEE FOR AERONAUTICS

986

. Inboard duct Area = 9.38 sq.in.					Outboard duct Area = 9.38 sq. in.				
	$\frac{Q_0}{F_0V_0} = 0.$	04/	Inlet I	nun	nber	/ 	$\frac{Q_0}{5V_0} = 0.$	047	
	9.86		95			0.97		0.93	
	9.86		0.96			0.96		0.94	
	0.84 0.86	0.95	96 .95		0.98	997	9.98	993.93	
	9.86		0.96	-		0.96		0.93	

0.96

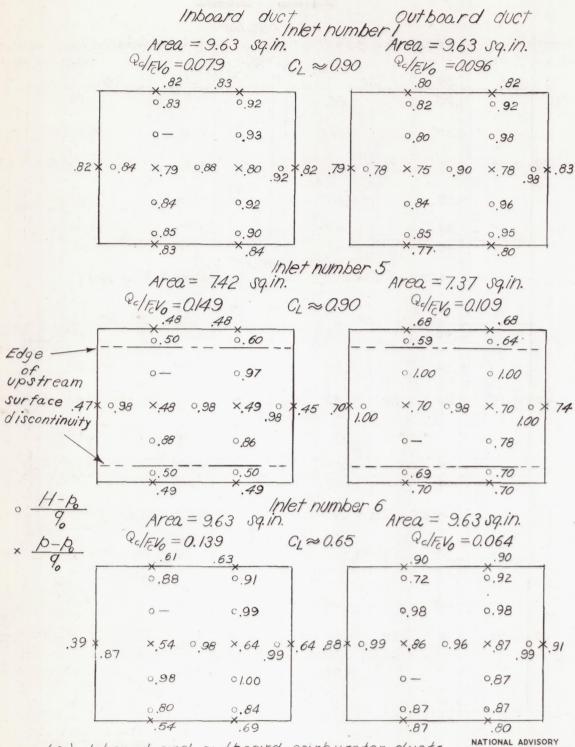
Qo EV	0 = 0.041	Inlet num	nber 5	$\frac{Q_0}{F_0V_0} = 0$	0.047
	9.80	0.93	0.96		°. <i>88</i>
	9.80	9.89	93		9.89
978	979 980	9.85 .95	0,96 0.92	9 <i>8</i> 8	°89 °
	9.80	9.84	0.92		0.88
	980	9.84	993		988

0.97

NATIONAL ADVISORY COMMITTEE FOR AERONAUTICS

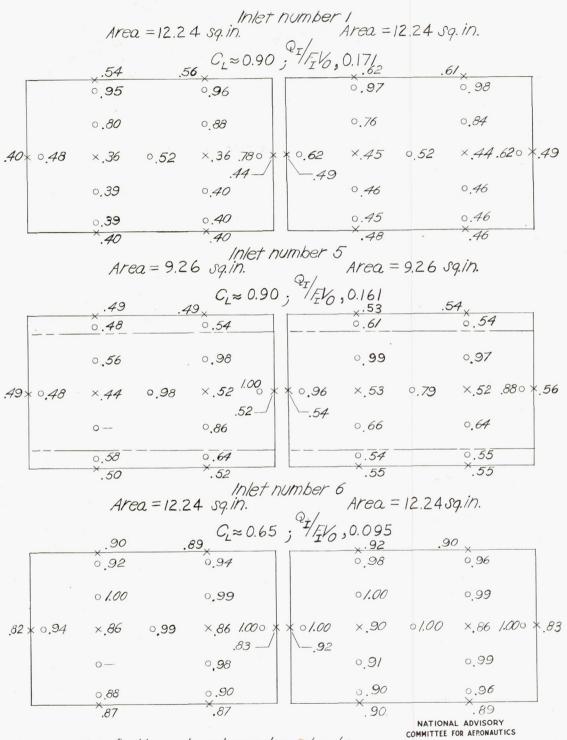
094

(d) Inboard and outboard oil-cooler ducts.
Figure 17. - Concluded.

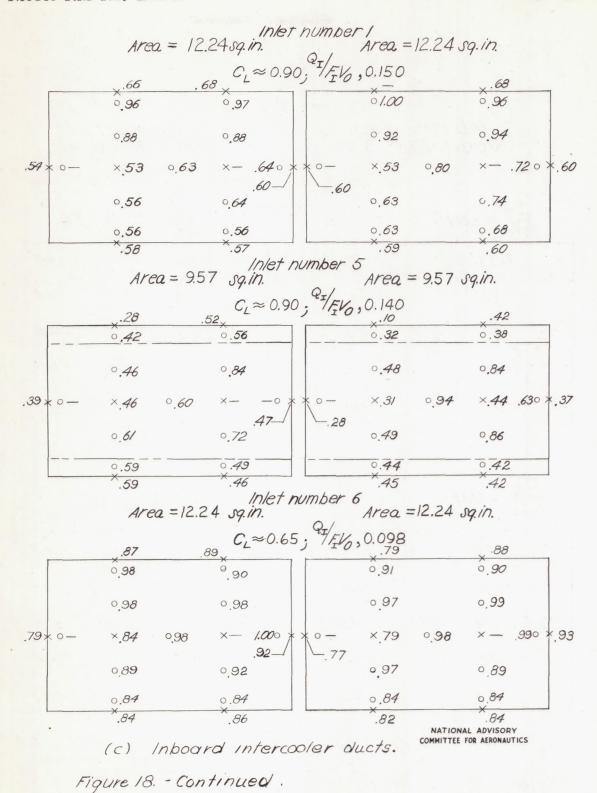


(a) Inboard and outboard carburetor ducts. COMMITTEE FOR AERONAUTICS

Figure 18. - Representative distributions of total and static pressure coefficients at measuring stations in ducting for the propeller-removed climb condition.



(b) Outboard intercooler ducts.
Figure 18. - Continued.



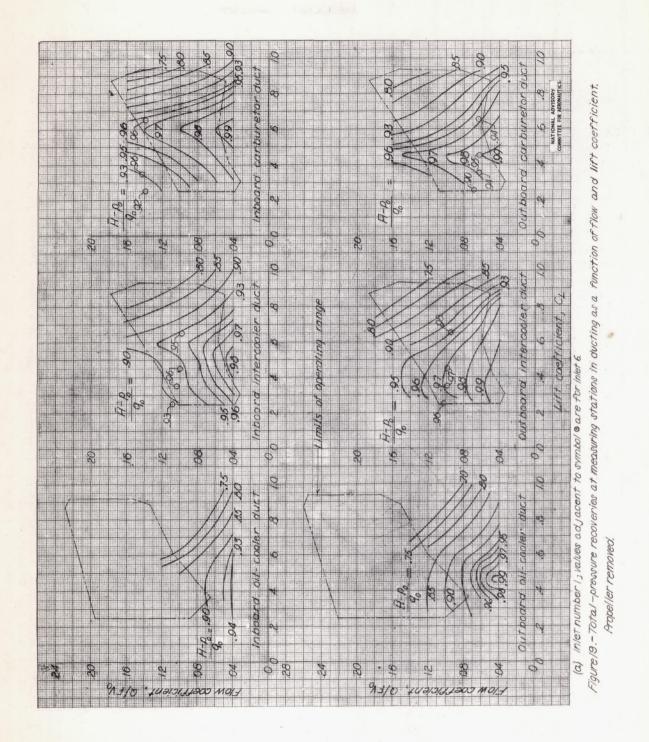
	Inboard duct Area = 9.38 sq.in.				Outboard duct Area = 9.38 sq.in.			
Fo	$\frac{20}{V_0} = 0.7$	119	Inlet n C <sub>L</sub> ≈			Qo FoVo	= 0./3	36
	0.33		0.68			0.58		0.44
	932		9.70			0.64		0.44
9.32	93/	937	.68°		97/	96 <b>6</b>	050	0.44.44
	0,3/		0.72	u.		967		0.42
	0.45		988			983		964

$\frac{Q_0}{f_0V_0} = 0.119$	Inlet num $C_L \approx 0$	Q
9.36	0.54	o.74 o.48
9.36	9.24	.56 ·.48
·25 ·34 ·41	°.43 ° .76	988 951 9.49 9.48 9 9.48
933	952	9.64 9.48
.29	0,52	9.81 9.49

(d) Inbourd and outboard oil-cooler ducts.

NATIONAL ADVISORY
COMMITTEE FOR AERONAUTICS

Figure 18. - Concluded.



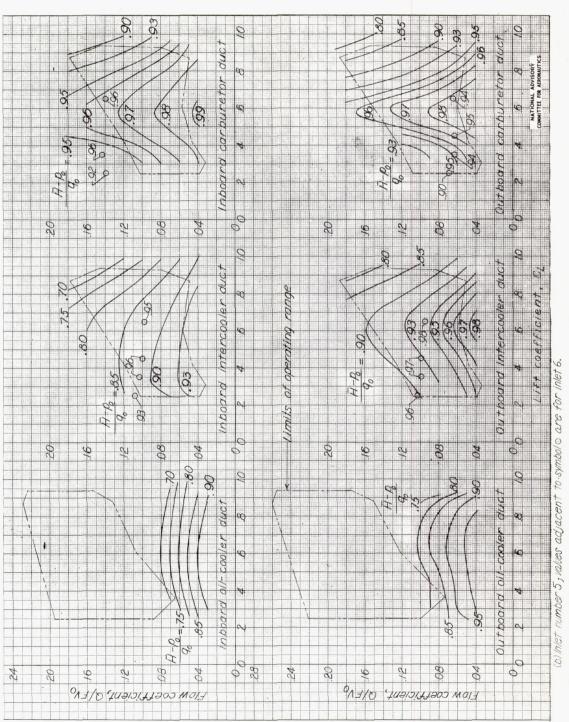
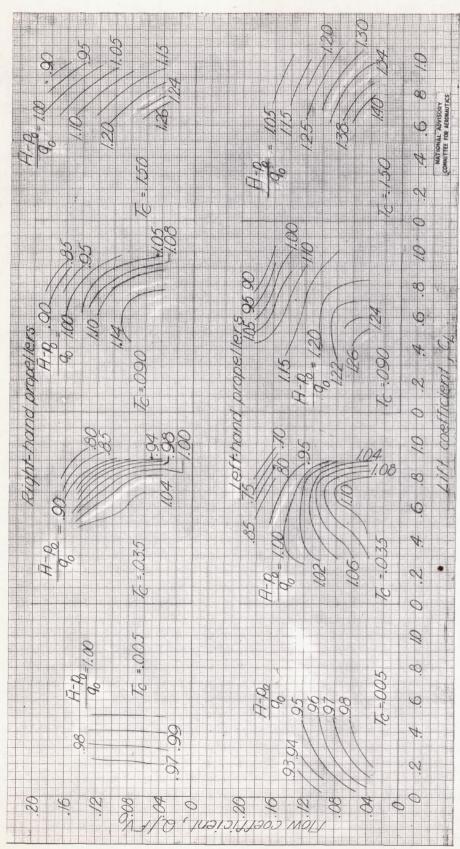


Figure 19. - Concluded.



of inlet on total-pressure coefficient in inboard intercooler duct operation